

AD-A138 571

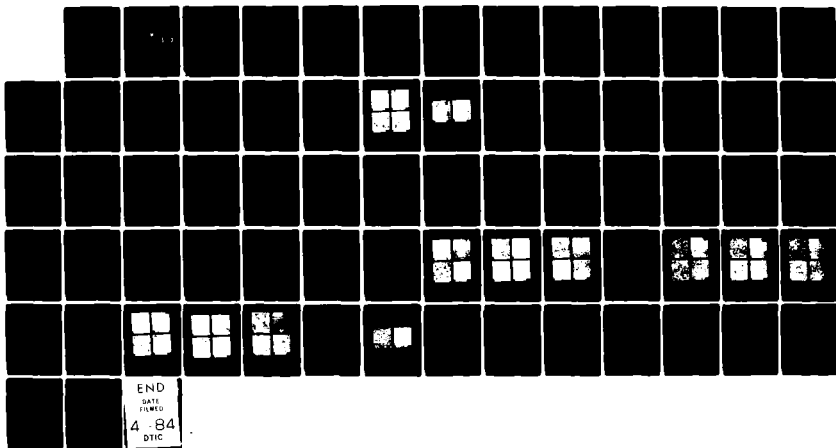
THE HEAT TREATMENT RESPONSE OF THERMOMECHANICALLY  
PROCESSED M-50 STEEL(U) NAVAL POSTGRADUATE SCHOOL  
MONTEREY CA E V BRES DEC 83

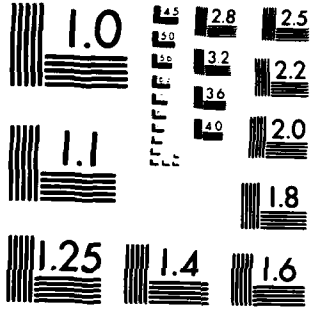
1/1

UNCLASSIFIED

F/G 11/6

NL





MICROCOPY RESOLUTION TEST CHART  
NATIONAL BUREAU OF STANDARDS-1963-A

2

# NAVAL POSTGRADUATE SCHOOL Monterey, California

AD A 138571



DTIC  
ELECTE  
MAR 6 1984  
S B D

## THESIS

THE HEAT TREATMENT RESPONSE OF  
THERMOMECHANICALLY PROCESSED M-50 STEEL

by

Elizabeth Vaughan Bres

December 1983

Thesis Advisor:

T. R. McNelley

Approved for public release; distribution unlimited.

DTIC FILE COPY

84 03 05 040

REPORT DOCUMENTATION PAGE		READ INSTRUCTIONS BEFORE COMPLETING FORM
1. REPORT NUMBER	2. GOVT ACCESSION NO. AD A138 571	3. RECIPIENT'S CATALOG NUMBER
4. TITLE (and Subtitle) The Heat Treatment Response of Thermomechanically Processed M-50 Steel		5. TYPE OF REPORT & PERIOD COVERED Master's Thesis; December 1983
7. AUTHOR(s) Elizabeth Vaughan Bres		8. CONTRACT OR GRANT NUMBER(s)
9. PERFORMING ORGANIZATION NAME AND ADDRESS Naval Postgraduate School Monterey, California 93943		10. PROGRAM ELEMENT, PROJECT, TASK AREA & WORK UNIT NUMBERS
11. CONTROLLING OFFICE NAME AND ADDRESS Naval Postgraduate School Monterey, California 93943		12. REPORT DATE December 1983
14. MONITORING AGENCY NAME & ADDRESS (if different from Controlling Office)		13. NUMBER OF PAGES 69
		15. SECURITY CLASS. (of this report) Unclassified
		15a. DECLASSIFICATION/DOWNGRADING SCHEDULE
16. DISTRIBUTION STATEMENT (of this Report) Approved for public release; distribution unlimited.		
17. DISTRIBUTION STATEMENT (of the abstract entered in Block 20, if different from Report)		
18. SUPPLEMENTARY NOTES		
19. KEY WORDS (Continue on reverse side if necessary and identify by block number) M-50 Fracture Heat Treatment Insoluble Carbides Microstructural Refinement Carbide Refinement Bearings Hardness Thermomechanical Processing Fatigue		
20. ABSTRACT (Continue on reverse side if necessary and identify by block number) The heat treatment response of M-50 steel, thermomechanically processed by warm rolling, was compared to that of the same material in a conventional, spheroidize-annealed condition. Warm rolling of M-50 produces markedly finer microstructures than does conventional processing, and may result in enhanced fracture resistance in such a steel. This work examined the effect of austenitizing time and temperature		

on warm rolled material, comparing its response to that of a conventional, spheroidized starting condition. Warm rolled samples demonstrated significantly higher hardness and retained their finer microstructures after short austenitizing times or treatment at low austenitizing temperatures. The hardness difference is attributed to faster dissolution of finer carbides. Using warm rolled M-50, a given hardness is achieved using shorter austenitizing times or lower austenitizing temperatures than for conventional M-50.

Accession For	
NTIS GRA&I	<input checked="" type="checkbox"/>
DTIC TAB	<input type="checkbox"/>
Unannounced	<input type="checkbox"/>
Justification _____	
By _____	
Distribution/	
Availability Codes	
Dist	Avail and/or Special
A1	



Approved for public release; distribution unlimited.

The Heat Treatment Response of  
Thermomechanically Processed M-50 Steel

by

Elizabeth Vaughan Bres  
Lieutenant, United States Navy  
B.S., Vanderbilt University, 1977

Submitted in partial fulfillment of the  
requirements for the degree of

MASTER OF SCIENCE IN MECHANICAL ENGINEERING

from the

NAVAL POSTGRADUATE SCHOOL  
December 1983

Author:

*Elizabeth V. Bres*

Approved by:

*Henry R. Milley*

Thesis Advisor

*Richard D. Chaffey*

Second Reader

*J. J. Marto*

Chairman, Department of Mechanical Engineering

*W. Dyer*

Dean of Science and Engineering

## ABSTRACT

The heat treatment response of M-50 steel, thermomechanically processed by warm rolling, was compared to that of the same material in a conventional, spheroidize-annealed condition. Warm rolling of M-50 produces markedly finer microstructures than does conventional processing, and may result in enhanced fracture resistance in such a steel. This work examined the effect of austenitizing time and temperature on warm rolled material, comparing its response to that of a conventional, spheroidized starting condition. Warm rolled samples demonstrated significantly higher hardness and retained their finer microstructures after short austenitizing times or treatment at low austenitizing temperatures. The hardness difference is attributed to faster dissolution of finer carbides. Using warm rolled M-50, a given hardness is achieved using shorter austenitizing times or lower austenitizing temperatures than for conventional M-50.

## TABLE OF CONTENTS

I.	INTRODUCTION .....	10
II.	EXPERIMENTAL PROCEDURE .....	20
	A. MATERIAL DESCRIPTION .....	20
	B. PREPARATION FOR HEAT TREATMENT .....	22
	C. HEAT TREATMENT .....	24
	D. HARDNESS TESTING AND MICROSCOPY .....	28
III.	RESULTS AND DISCUSSION .....	31
	A. HARDNESS AND CARBIDE SOLUTIONING .....	31
	B. MICROSTRUCTURAL RESULTS .....	45
	C. COMPARISON OF WARM ROLLING AND AUSFORMING .....	61
IV.	CONCLUSIONS AND RECOMMENDATIONS .....	65
	LIST OF REFERENCES .....	67
	INITIAL DISTRIBUTION LIST .....	69

LIST OF TABLES

I.	Characteristic Parameters for M-50 Steel -----	17
II.	Material Properties for M-50 Steel Warm Rolled at 700C -----	21
III.	Hardness Test Results for Two Minute Austenitizing Time -----	34
IV.	Hardness Test Results for 1020C Austenitizing Temperature -----	35
V.	Hardness Test Results for 1120C Austenitizing Temperature -----	36

## LIST OF FIGURES

1.	Trend in Aircraft Engine Main Bearing DN. -----	11
2.	Bearing Spalling and Rapid Fracture. -----	12
3.	Comparison of As-received and Warm Rolled M-50 by Optical Microscopy. -----	18
4.	Comparison of As-received and Warm Rolled M-50 by Scanning Electron Microscopy. -----	19
5.	Optical Microscopy Specimen Preparation. -----	22
6.	Heat Treatment of Warm Rolled M-50. -----	26
7.	Heat Treatment of As-received M-50. -----	27
8.	Results of Microhardness Traverses of the Long and Short Axes of Warm Rolled and As-received M-50, Austenitized Two Minutes at 900C. -----	32
9.	Hardness of Warm Rolled and As-received M-50 at Austenitizing Time Two Minutes, Varying Austenitizing Temperature. -----	37
10.	Hardness of Warm Rolled and As-received M-50 at Austenitizing Temperature 1020C, Varying Austenitizing Time. -----	38
11.	Hardness of Warm Rolled and As-received M-50 at Austenitizing Temperature 1120C, Varying Austenitizing Time. -----	39
12.	Hardness of Warm Rolled M-50 at Austenitizing Temperature 1120C, Varying Austenitizing Time. -----	40
13.	Hardness of As-received M-50 at Austenitizing Temperature 1120C, Varying Austenitizing Time. -----	41
14.	Comparison of Microstructures Resulting After Heat Treatment of As-received and Warm Rolled M-50 at Austenitizing Temperatures of 900C and 1000C (Optical Microscopy, 320x). -----	47

15.	Comparison of Microstructures Resulting After Heat Treatment of As-received and Warm Rolled M-50 at Austenitizing Temperatures of 1050C and 1100C (Optical Microscopy, 320x). -----	48
16.	Comparison of Microstructures Resulting After Heat Treatment of As-received and Warm Rolled M-50 at Different Austenitizing Temperatures (Optical Microscopy, 800x). -----	49
17.	Comparison of Microstructures Resulting After Heat Treatment of As-received and Warm Rolled M-50 for Short Austenitizing Times at 1020C (Optical Microscopy, 320x). -----	51
18.	Comparison of Microstructures Resulting After Heat Treatment of As-received and Warm Rolled M-50 for Long Austenitizing Times at 1020C (Optical Microscopy, 320x). -----	52
19.	Comparison of Microstructures Resulting After Heat Treatment of As-received and Warm Rolled M-50 for Different Austenitizing Times at 1020C (Optical Microscopy, 800x). -----	53
20.	Comparison of Microstructures Resulting After Heat Treatment of As-received and Warm Rolled M-50 for Short Austenitizing Times at 1120C (Optical Microscopy, 320x). -----	56
21.	Comparison of Microstructures Resulting After Heat Treatment of As-received and Warm Rolled M-50 for Long Austenitizing Times at 1120C (Optical Microscopy, 320x). -----	57
22.	Comparison of Microstructures Resulting After Heat Treatment of As-received and Warm Rolled M-50 for Different Austenitizing Times at 1120C (Optical Microscopy, 800x). -----	58
23.	Comparison of Microstructures Resulting After Heat Treatment of As-received and Warm Rolled M-50 for Austenitizing Time 12 Seconds at 1120C (Optical Microscopy, 320x). -----	60
24.	Time-Temperature-Transformation Diagram for M-50 Steel. -----	62

## ACKNOWLEDGEMENTS

I would like to express my very great appreciation for the guidance and encouragement provided by my thesis advisor, Professor Terry R. McNelley. Mr. Tom Kellogg's technical expertise and unfailing patience and good humor were also essential to the successful completion of this work, and thanks are due to LT Linda C. Janikowsky, USN, for her unsurpassed critical eye.

This work is supported by the Naval Air Propulsion Center, Trenton, NJ, as part of its program directed at improved bearing materials. I am grateful to Mr. Dan Popgoshev, of that command, for his valuable comments and suggestions.

## I. INTRODUCTION

Aircraft engine designs now being developed will require better bearing materials than available today. Early gas turbine engine performance was most severely restricted by the temperature limits imposed by the blade materials. Since both specific fuel consumption and power are improved by increased turbine inlet temperatures, there was incentive for extensive research, and this led to blade alloys matching the extremely harsh criteria imposed by modern engine operating conditions. At the elevated temperature made possible with these materials, increasing turbine speed boosts performance, while a multi-spool configuration enhances efficiency. These innovations have shifted research attention to the problem of larger, higher speed bearings now required.

Trends in bearing parameters may be described by using the DN number. Bore diameter,  $D$ , in millimeters, is increased by a multi-spool engine's larger shaft. Diameter is multiplied by  $N$ , the shaft rotations per minute. The roughly linear increase in this measure over time is illustrated by Figure 1 [Ref. 1].

Bearing DN has been linked to the expected bearing failure mode. At lower DN (up to about 2 million), the classical mode of failure for a properly installed and maintained

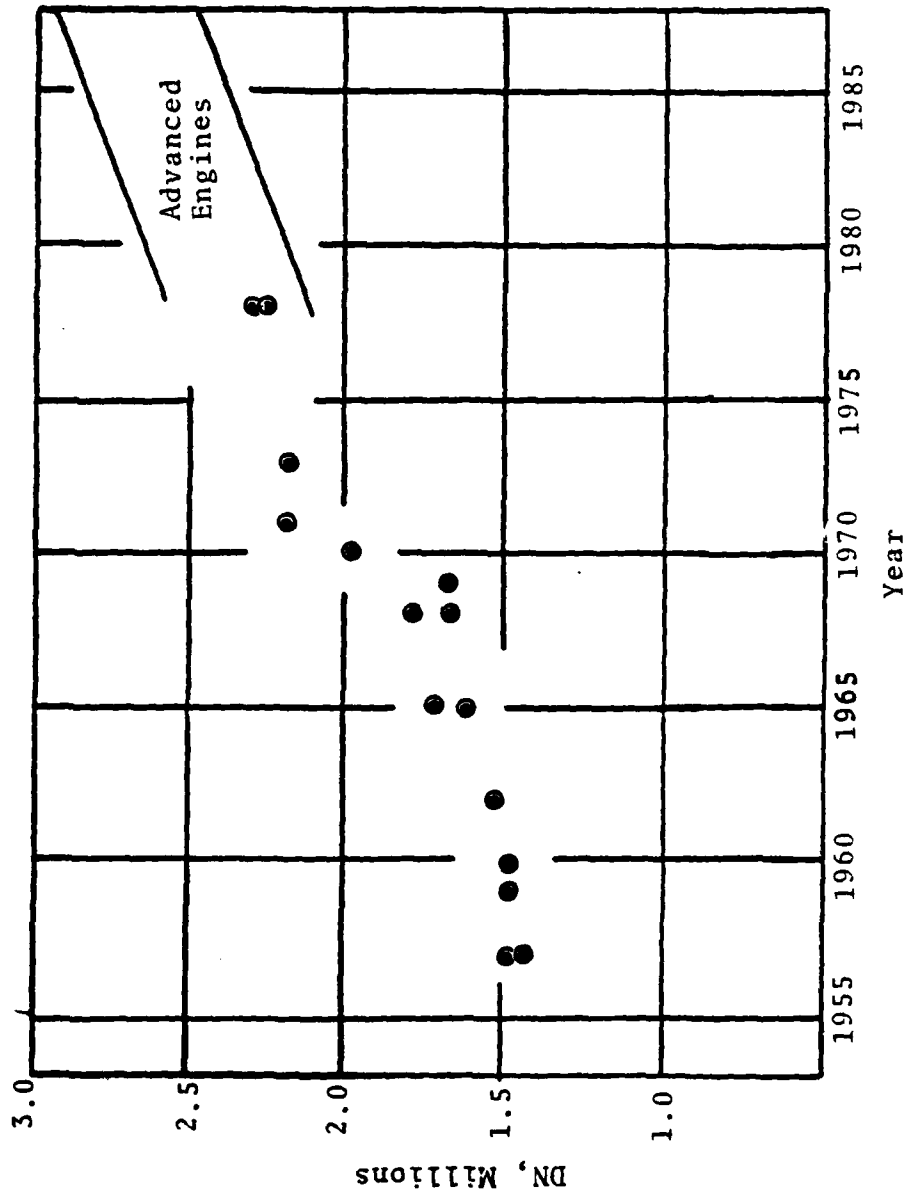


Figure 1. Trend in Aircraft Engine Main Bearing DN.

bearing is spalling due to rolling contact fatigue in a Hertzian stress field [Ref. 2]. Spalling, the inner surface chipping resulting from the propagation of subsurface flaws or cracks (Figure 2), is a relatively slow process, and it is usually possible to identify and replace failed bearings before they cause engine damage.

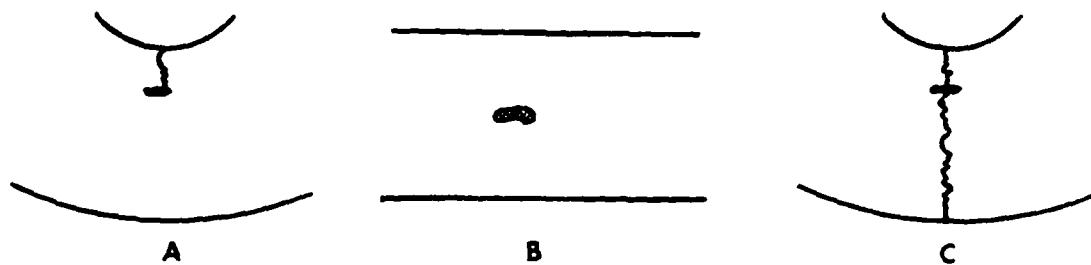


Figure 2. Bearing Spalling and Rapid Fracture. A) Spalling initiates from a subsurface flaw or crack and propagates to the inner surface. B) The spall itself is a chip on the raceway surface. C) Rapid fracture initiates at a subsurface flaw or crack and propagates in two directions.

High DN values result in high hoop and frictional stresses, with the result that the expected mode of failure shifts to

catastrophic rapid fracture [Ref. 3]. Averbach, with others [Refs. 4,5], has demonstrated how linear elastic fracture mechanics may be applied to analyze and predict the behavior of a rolling element bearing of known fracture toughness in a given combination of Hertzian, hoop, and frictional stresses.

An important factor in reliable performance at high DN lies in improving the fracture toughness of the bearing material without a concurrent sacrifice in the hardness essential for wear resistance and long rolling contact fatigue life. Development of high toughness, high strength bearing materials is critical to the next generation of gas turbine engines, and can also provide an added margin of safety for the operation of existing designs.

While most strategies to improve fracture toughness do so at the expense of strength, microstructural refinement yields beneficial changes in both properties by fighting fracture in two ways [Ref. 6]. First, pre-existing cracks in the material are expected to be smaller, which raises the stress required to propagate them to fracture. This effect is described by the relationship

$$K_{IC} = \sigma_f \sqrt{\pi a}$$

where  $K_{IC}$  is the critical stress intensity factor (fracture toughness),  $\sigma_f$  is the applied stress at fracture, and  $a$  is the characteristic crack length. Since  $K_{IC}$  is a material

constant, it is evident that a smaller crack requires larger applied stress for fracture to result.

Secondly, the increased grain boundary area in a finer structure increases the number of obstacles in a propagating crack's path. Conventional processing of bearing steel emphasizes the need to devise heat treatment schemes to give minimum grain size at required hardness levels [Ref. 7]; unfortunately, testing has shown that the fracture toughness levels resulting from current heat treatment cycles are inadequate for roller bearings operating at high DN [Ref. 8].

Microstructural refinement may be achieved through an innovative method known as "warm rolling" developed at Stanford University by Sherby et al. [Refs. 9,10]. By working plain carbon steels just below the eutectoid temperature, Sherby produced materials which were superplastic at temperatures between 0.5 and 0.65 of the absolute melting temperature. Plastic deformation during a spheroidizing anneal was observed to speed spheroidization and reduce the interparticle spacing. The shorter interparticle spacing is a consequence of carbide nucleation at the dislocation tangles generated by the rolling. The resulting ultrafine dispersion of carbides in a ferrite matrix meets the prerequisites for superplasticity: very fine, stable, equiaxed grains, two phases of roughly equal strength at warm temperature, and high strain rate sensitivity. A superplastic material is

very easily formed - elongation may exceed 500% [Ref. 10] - which would facilitate bearing component fabrication.

Steels in the warm rolled condition are too soft to be used in bearings. If the finer microstructure is retained through a subsequent hardening heat treatment it might offer a significant fracture toughness advantage. Sherby warm rolling has been applied to AISI 52100 steel, to test the method's efficacy for bearing applications [Ref. 11]. Warm rolled, finely spheroidized 52100 and standard material were both conventionally hardened and isothermally transformed. The warm rolled steel's finer carbide size and more uniform microstructure were retained after heat treatment. For identical conventional heat treatments, warm rolled steel was at least as hard as standard 52100. When compared at equal strengths, fracture toughness was found to be higher for the warm rolled product (again after conventional treatment) than for the standard 52100, as expected for a finer microstructure.

Based on the favorable outcome of the 52100 study, a series of experiments was initiated to seek similar improvements in the fracture toughness of AISI M-50, the standard bearing steel for high performance gas turbine engines manufactured in the United States. The application of M-50 in this role is due to its ability to resist softening even on prolonged exposure to temperatures up to 350F (175C). Larson [Ref. 12] successfully warm rolled M-50 in the 650-750C

temperature range. He observed highly refined  $M_{23}C_6$  and  $M_6C$  carbides in a refined ferrite matrix, with insoluble  $M_2C$  and  $MC$  carbides slightly smaller than they occur in as-received M-50. The warm rolled material had higher ultimate tensile strength when compared to steel in the spheroidize-annealed condition as it is received from the manufacturer. The difference in strength depended primarily on the temperature at which the steel was rolled; the effect on strength of austenitizing temperature was not significant. Quantitative differences between the two starting conditions are indicated in Table I for a typical warm rolling preparation, and qualitative differences may be seen in Figures 3 and 4.

In addition, Bridge, Maniar and Phillip's findings of two distinct insoluble carbides, one molybdenum rich, the other mostly vanadium [Ref. 13], was confirmed. The present research compared warm rolled M-50's response to heat treatment to that of the standard spheroidized starting condition. Two experiments were undertaken. In the first, austenitizing temperature varied at constant time, while the second held austenitizing temperature constant over a series of times. After quenching, hardness and microstructure were examined.

TABLE I  
Characteristic Parameters for M-50 Steel

<u>Alloy Condition</u>	<u>Tensile Strength (Ksi)</u>	<u>Tensile Strength (MPa)</u>	<u>Soluble Carbide Size (Microns)</u>	<u>Insoluble Carbide Size (Microns)</u>	<u>Percent Elongation</u>
As-received	100.1	690.1	0.5 - 3.0	3-18	22
Aust. 1180C (5 hr) Warm rolled 700C	150.9	1049.4	<0.1 - 1.0	1-10	8

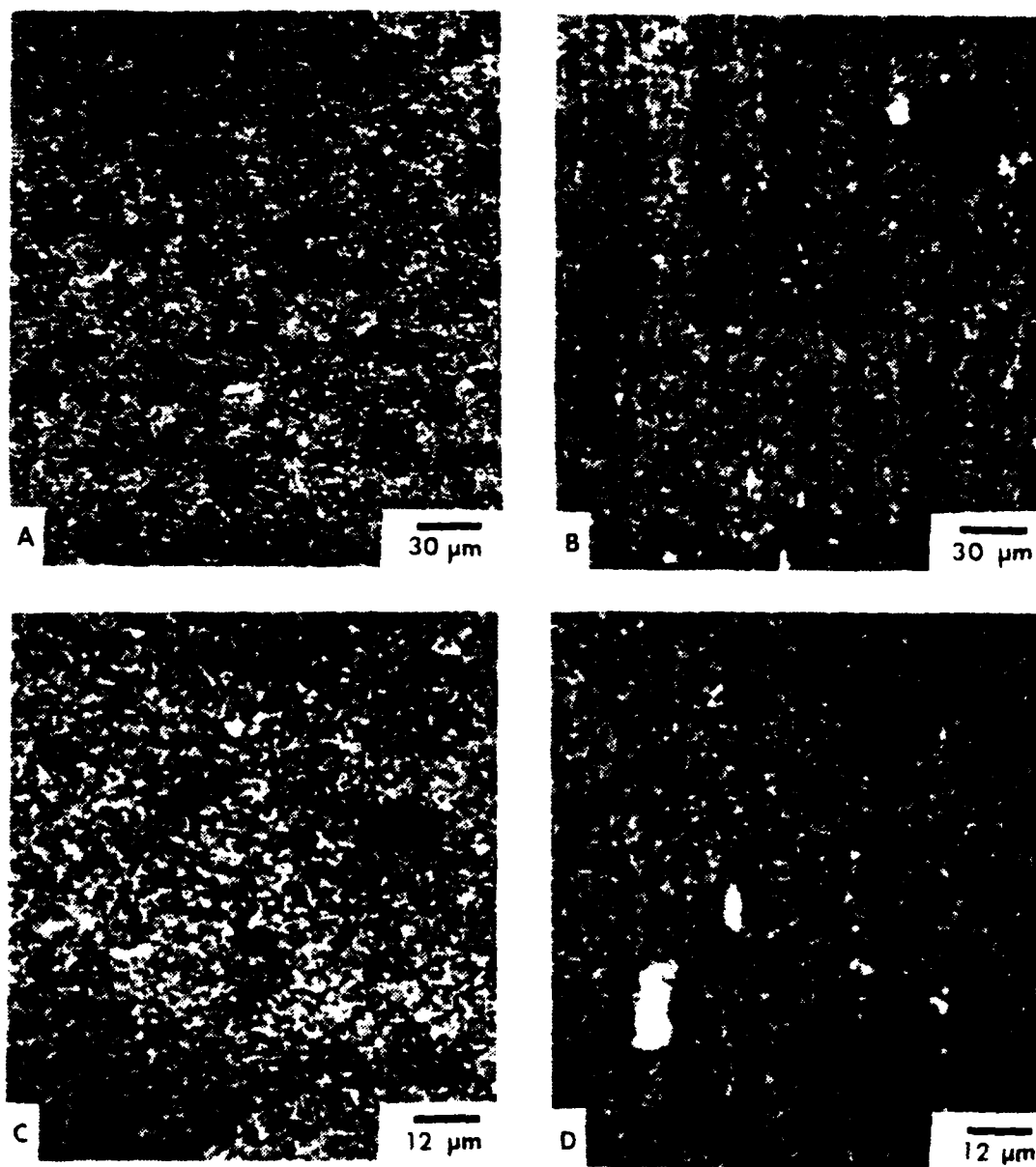


Figure 3. Comparison of As-received and Warm Rolled M-50 by Optical Microscopy. A) As-received, 320x. B) Warm rolled, 320x. C) As-received, 800x. D) Warm rolled, 800x. Light areas are insoluble carbides in all cases. The dark areas in A and B are unresolved carbides. In C, the carbides of the as-received material are resolved while those in the warm rolled steel are not (D). Grain size was not revealed by this etch.

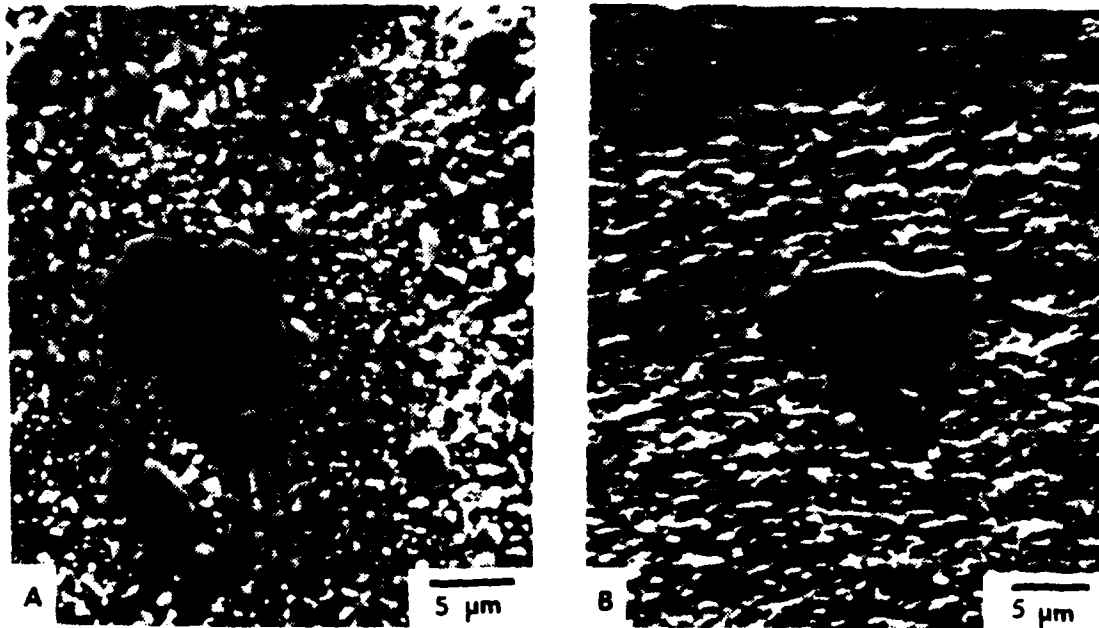


Figure 4. Comparison of As-received and Warm Rolled M-50 by Scanning Electron Microscopy. A) As-received, 2400x. [Ref. 12] B) Warm rolled at 700C, 2200x. [Ref. 12] Large insoluble carbides are not greatly reduced by warm rolling, but small soluble carbides are significantly refined.

## II. EXPERIMENTAL PROCEDURE

### A. MATERIAL DESCRIPTION

The nominal amounts of alloying elements in M-50 are

C	Mo	Cr	V	Mn	Si
0.8	4.0	4.0	1.0	0.3	0.25

Two starting conditions for heat treatment were compared in this research; all test coupons, whether in the as-received condition or warm rolled, came from the same heat of steel.

Material in the warm rolled condition used for this study was processed by Larson [Ref. 12], who reported that the effect on microstructural refinement austenitizing temperature prior to warm rolling was not significant when compared to the effect of the rolling temperature. Consequently, all material rolled by Larson at 700C was considered identical, regardless of the initial austenitizing temperature. Mechanical properties of the four austenitizing time and temperature combinations used in the experiments were comparable, as shown in Table II.

The as-received material used in this research had a hardness of 95 HRB before heat treatment; other properties are listed in Table I.

TABLE II  
Material Properties of M-50 Steel Warm Rolled at 700C

<u>Austenitizing Temperature(C)</u>	<u>Austenitizing Time</u>	<u>Percent Elongation</u>	<u>Tensile Strength (Ksi)</u>	<u>Tensile Strength (MPa)</u>	<u>Hardness (Rockwell C)</u>
1180	3 x 1 hr	7	153.4	1057.6	33
1180	5 hr	8	150.9	1040.4	35
1180	1 hr	11	143.4	988.7	31
1100	5 hr	10	140.3	988.0	31

## B. PREPARATION FOR HEAT TREATMENT

The important steps in the preparation and heat treatment of M-50 test coupons are shown in Figure 5.

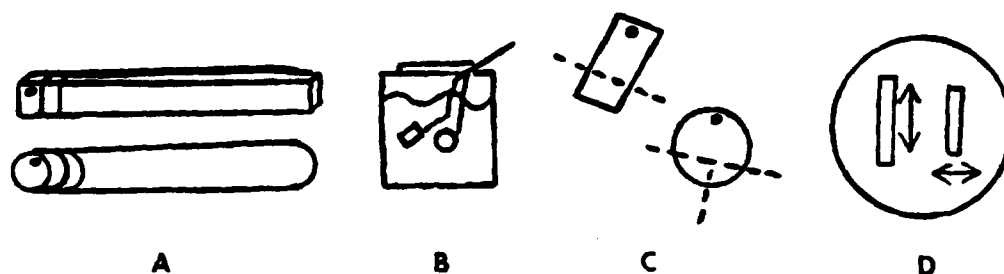


Figure 5. Optical Microscopy Specimen Preparation. A) Sections cut from warm rolled material (top) and one-inch round stock (bottom) and drilled. B) Heat treatment in salt baths; specimens wired to thermocouples. C) Samples cut for mounting. D) Face of finished bakelite mount. Arrows show long axis of original stock. Vertical arrow indicates sample processed from warm rolled material and horizontal arrow shows orientation of sample processed directly from the spheroidized annealed condition.

Test coupons were cut from lengths of warm rolled M-50 and from one-inch (25 mm) round stock as provided by the manufacturer. Coupons in both cases were about 2.5 mm (0.1 inch) thick. The whole diameter of the round stock was used, while the warm rolled steel, which was approximately one inch wide, was cut into 1.3 mm (0.5 inch) lengths. Each coupon was drilled in order to permit the coupon to be held by a wire during heat treatment.

A heat treatment rig was fabricated based on two Type K (Chromel-Alumel) Inconel 600 sheathed thermocouples. The quick disconnect fittings of the thermocouples were placed

one on top of the other and wired together to secure them in that position. Each thermocouple was bent about one inch from its tip to an angle of about  $100^{\circ}$ . Fine nichrome wire was passed through the drilled hole in a test coupon, then the coupon was held on the bent end of the thermocouple and the wire wrapped around the thermocouple and coupon to make and maintain contact between the two components. For each austenitizing condition (i.e., each combination of austenitizing time and temperature), one thermocouple held a warm rolled test coupon, while the other held a coupon in the as-received condition (Figure 5B).

Using the thermocouples themselves as the framework for the test rig had three advantages. First, it made the rig easy to hold while wearing cumbersome protective gloves, and so made quick transfers possible between the pre-heat, austenitize, and quench salt baths. Second, it ensured that both the as-received and warm rolled test coupons would be in the same general location of each salt bath, but without touching each other, so that coupons tested together received identical heat treatments. Last, it allowed constant monitoring of the test coupon temperatures.

Two difficulties arose with this test assembly. The Type K thermocouples, while accurate to  $1260^{\circ}\text{C}$ , were embrittled at high temperatures and therefore broke very easily when attaching and removing samples. Platinum-rhodium thermocouples should be used when temperatures

being studied exceed 1100C. Also, temperature data from the thermocouples was logged by hand from two channels of a digital readout thermometer. Flipping the channel selector knob was inconvenient; the process could very easily be refined by using a multichannel strip chart or small computer for data collection.

### C. HEAT TREATMENT

The heat treatment of each pair of samples was conducted using three Lindberg model 56953 salt baths of about one liter capacity, one for pre-heating, one for austenitizing, and one for quenching the test coupons. Heat treatment was carried out in salt baths rather than in a furnace to take advantage of molten salts ability to provide heat to a test coupon at a rate equal to the heat absorption rate of the steel. The result is uniform heating of the sample. Salts used in the baths were Holden Annealing 975 for pre-heat and quenching, and Calalloy 1724 for the austenitizing bath.

Preheating and quenching were each the same for every treatment, at 850C and 620C respectively. Both the pre-heating and salt quenching were always of six minutes' duration. Following the salt quench the test coupons were air cooled until they could be handled without gloves, about 15 minutes.

The heat treatment variables were austenitizing temperature and time. Type K thermocouples are accurate up to

1260C, while Larson found partial melting of M-50 at 1200C [Ref. 12], and Inconel 600 embrittlement begins at around 1100C. The highest austenitizing temperature studied was 1150C, above that at which the thermocouple sheath would begin to embrittle, because standard heat treatment is conducted at around 1120C. Somewhat arbitrarily, 900C was selected as the lowest austenitizing temperature. It is substantially below the standard heat treatment range of 1081-1106C in salt [Ref. 15], and gives an adequate number of data points at conveniently spaced 50C intervals. The standard austenitizing time for this study was taken as two minutes, based on the industry rule of thumb of one hour's soak per inch of thickness of the workpiece.

The first experiment held austenitizing time constant and varied austenitizing temperature at nominal 50C increments. Typical heat treatments are illustrated schematically in Figures 6 and 7, for warm rolled and as-received materials, respectively. The left side of Figure 6 (time scale in hours) shows Larson's pre-roll austenitizing and warm rolling, in contrast to the left side of Figure 7, which shows the manufacturer's spheroidizing annealing treatment. The arrow in Figure 7 indicates the point at which standard processing is interrupted, in effect, for warm rolling. Note that this interruption occurs before the bearing would be fabricated. The right sides of both Figures 6 and 7 (time scale in minutes) show an austenitize and quench treatment typical of this experiment.

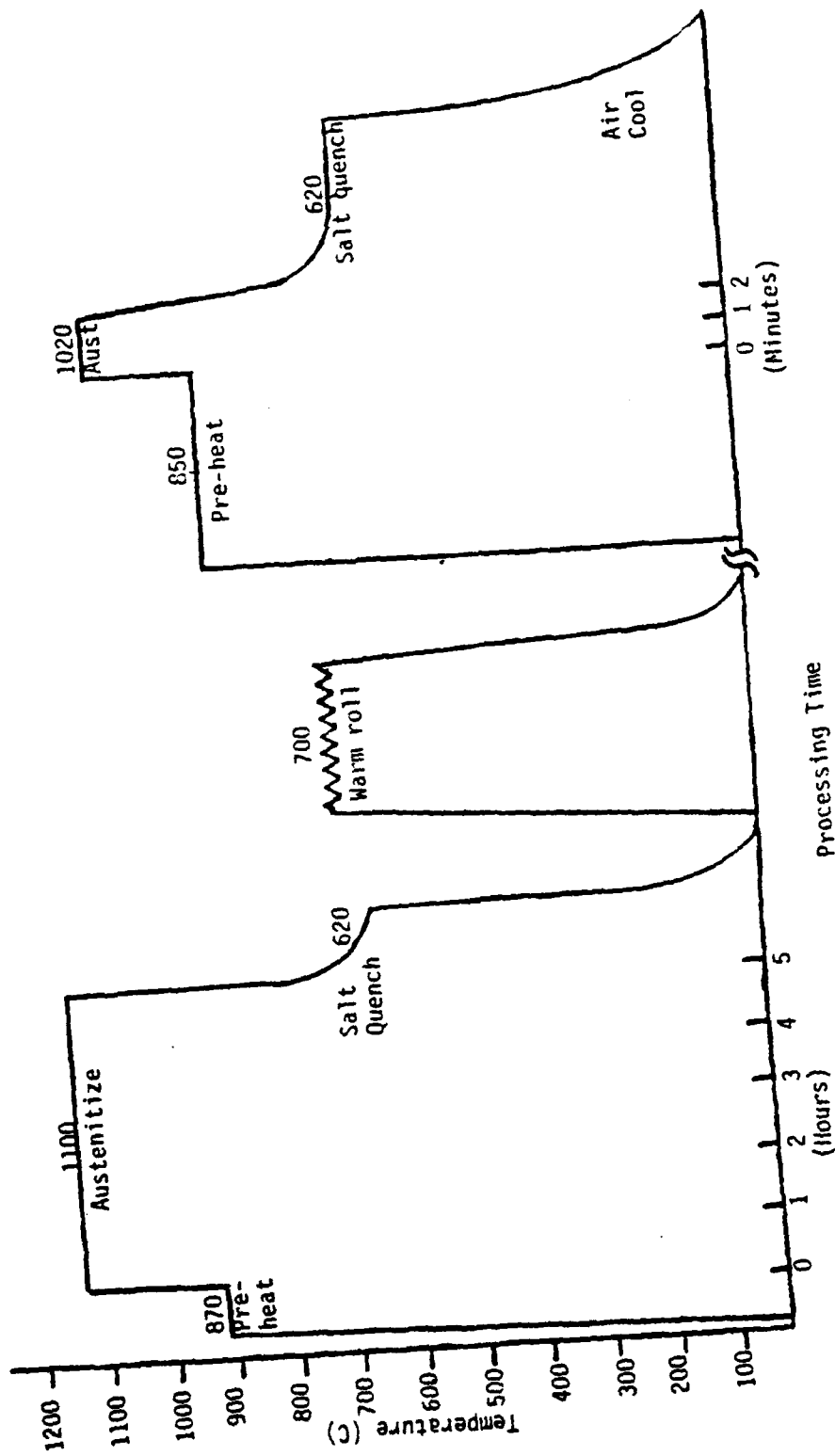


Figure 6. Heat Treatment of Warm Rolled M-50. The left side (time scale in hours) shows a typical austenitize and quench combination used to back the mar-tensitic structure. The right side (time scale in minutes) depicts a heat treat-ment typical of those studied.

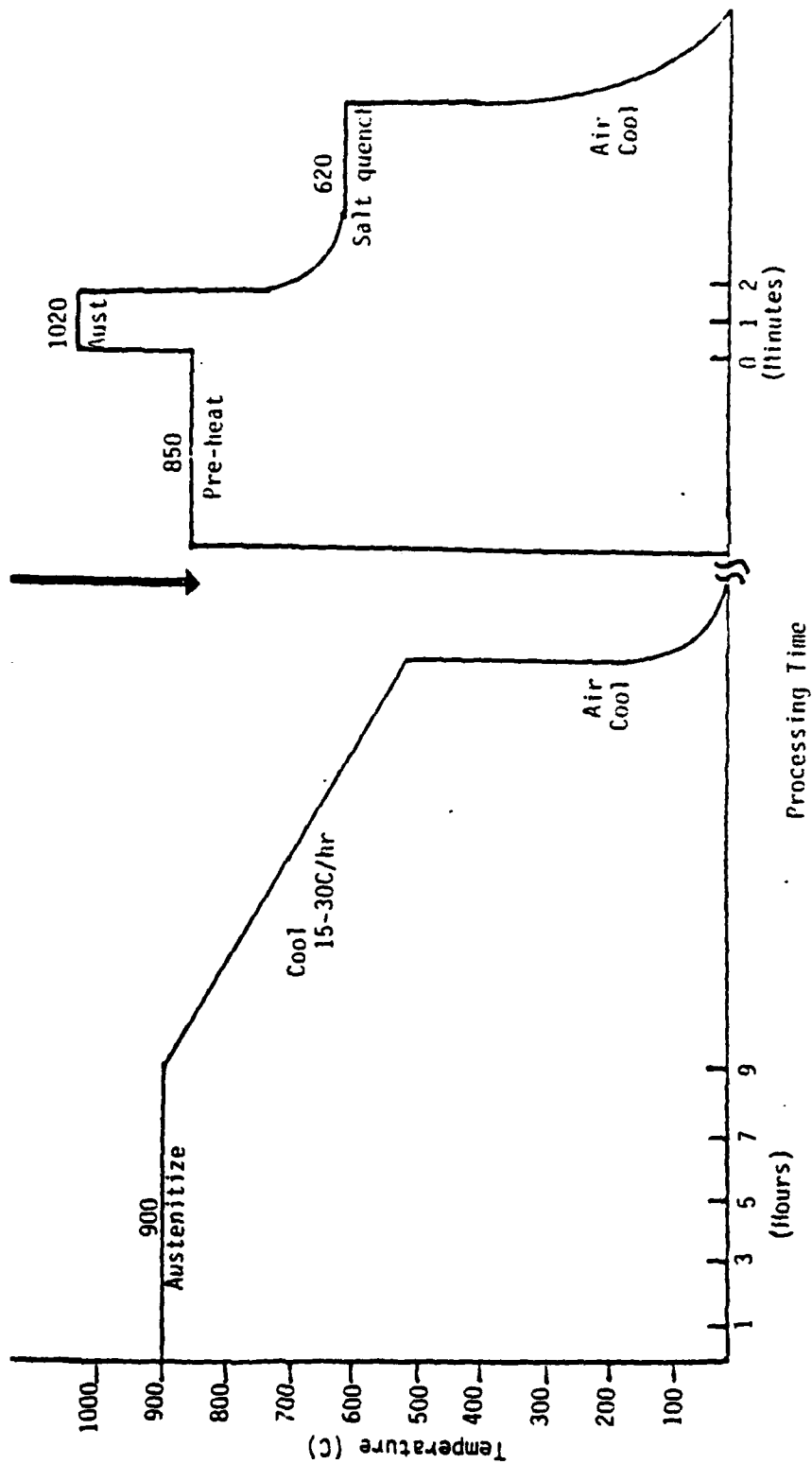


Figure 7. Heat Treatment of As-received M-50. The left side (time scale in hours) illustrates processing by the manufacturer, while the right side (time scale in minutes) is a heat treatment typical of those studied. The arrow indicates the point at which standard processing is interrupted, in effect, for warm rolling (left side of Figure 6).

After removal from the test rig, coupons were washed in warm running water to remove the salt residue. Grinding followed, using 80 and 180 grit papers on a belt grinder to remove a corroded surface layer and give a smooth, bright surface for hardness testing.

A second experiment examined the effects of varying the austenitizing time at each of two constant austenitizing temperatures, 1020C and 1120C. These temperatures were chosen to provide additional data points for the two minute austenitizing series and to illustrate the interaction of finer microstructure with time in two different carbide regimes, above and below the  $M_6C$  solidus temperature. In addition, 1120C is the standard heat treatment temperature for M-50. Test coupons, test rig, and preparation for hardness testing for this experiment are all identical to those described for the constant time experiment.

#### D. HARDNESS TESTING AND MICROSCOPY

Hardness measurements were made before and after heat treatment using a Wilson Rockwell Hardness Tester, Model 1JR, and the Rockwell C scale (the sole exception is in the case of measuring the hardness of the as-received steel before heat treatment, for which it was necessary to use the Rockwell B scale). Five indentations were made in each test coupon, according to ASTM Standard E 18-74 [Ref. 16]. The mean hardness and standard deviation were calculated for each coupon tested.

When hardness measurements were complete, test coupons from both experiments were sectioned using a Buehler Model 10-1010 Cut-Off Machine and a wafering wheel (Buehler designation "R"), then mounted in bakelite in pairs as they were tested together (Figures 5C and 5D). Specimens were ground using 80, 180, 240 and 400 grit abrasive papers on belt grinders, then polished on a series of wheels charged with 15, 6, 1, and 1/4 micron diamond paste.

Polished specimens were prepared for optical microscopy by etching in Villela's reagent [Ref. 17], modified by changing the amount of ethanol used from 100 to 200 milliliters. Quantities of hydrochloric acid and picric acid dissolved in the ethanol were unchanged at 5 milliliters and 1 gram, respectively. The formula for the reagent was altered in order to give better control of etching times, which were extremely short using the standard quantity of wetting agent. All etching was carried out at room temperature. Etching times varied from 3 to 23 seconds, depending in part on the age of the etchant mixture, but no clear relationship was discovered between etching time and any other variable. Prior austenite grain boundaries were not usually revealed, although Villela's reagent and similar picric acid etchants are recommended for this purpose [Refs. 18,19].

Data on uniformity of hardening and through hardening was obtained by making a microhardness traverse of one mounted specimen using Buehler Micromet Micro Hardness Tester (M-11) with 200 gram weight.

A Zeiss Universal microscope was used to examine the polished and etched microstructures. Thirty-five millimeter black and white photographs were taken using a halogen light source. After microstructures were documented optically at 320 and 800x, selected specimens were lightly repolished (1 minute on each of the 6, 1, and 1/4 micron diamond wheels), and etched for 10 seconds in the modified Villela's reagent. After being broken free of the bakelite, the specimen pairs were mounted with silver paste to large stubs for examination by scanning electron microscopy.

### III. RESULTS AND DISCUSSION

#### A. HARDNESS AND CARBIDE SOLUTIONING

Microhardness testing was conducted on samples of both warm rolled and as-received materials that were austenitized at 900C. This testing was conducted to evaluate the uniformity of hardening for the two processing conditions. The microhardness traverses, Figure 8, indicate that warm rolled M-50's hardness is more uniform than that of the as-received steel, as reflected by a difference of 48 hardness units between the highest and lowest value for warm rolled M-50 measured along the long axis. By comparison, as-received M-50 shows a range of 71 units when measured in the same direction. This result suggests that the warm rolled material is slightly more homogeneous than the as-received. Average hardnesses of 644HV (long axis, warm rolled) and 491 (long axis, as-received), may be converted to the Rockwell C scale by using ASTM Standard E 140-72 [Ref. 20]. The converted numbers, 57 HRC (warm rolled) and 48 HRC (as-received), compare well with the surface hardnesses measured with the Rockwell Hardness Tester: 56 HRC (warm rolled) and 48 HRC (as-received). Although the interior hardness of the warm rolled M-50 is very slightly higher, it may be concluded that the steel was uniformly through hardened since this value is not significantly different when the error in

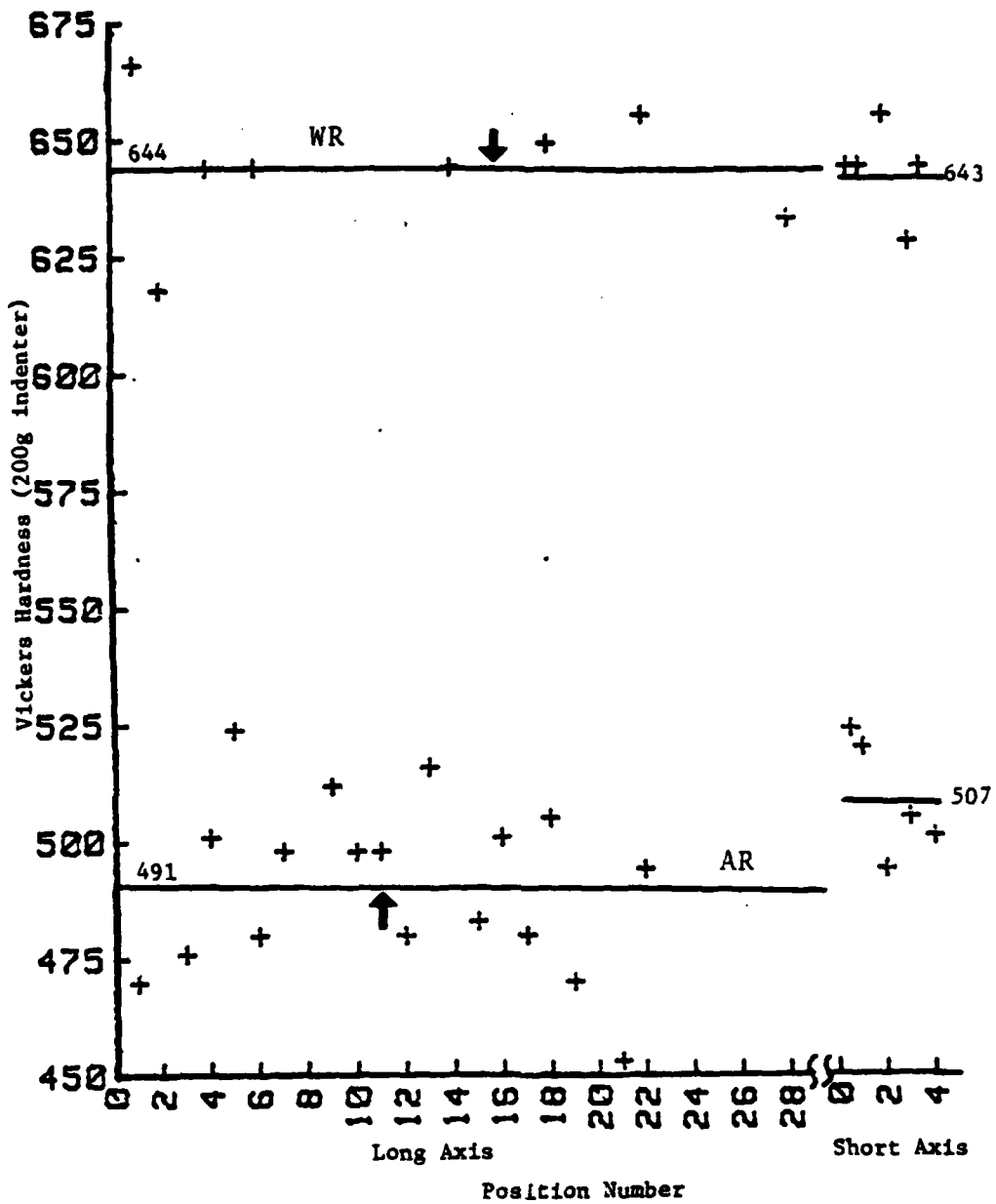


Figure 8. Results of Microhardness Traverses of the Long and Short Axes of Warm Rolled and As-Received M-50, Austenitized Two Minutes at 900C. Horizontal axis indicates points at which indentations were made; scale is in increments of  $\frac{1}{2}$  mm from the edge of the specimen. Solid lines mark the average hardness, and arrows indicate the positions at which the short axis traverses were made.

hardness measurement is considered ( $\pm 1/2$  HRC unit), and no evidence of decarburization was seen when the specimen was examined by optical microscopy at 800x.

Tables III-V and Figures 9-13 summarize the results obtained in the examination of the effects of austenitizing time and temperature. Figure 9 is data for the effect of austenitizing temperature, while Figures 10-13 are concerned with the effects of heating time. These data clearly show that heat treatment of warm rolled M-50 yields a product that is always at least as hard as the standard steel. At shorter austenitizing times, or for lower austenitizing temperatures, warm rolled material is significantly harder than the as-received steel given identical heat treatment. The graphs also show that, again for shorter austenitizing times or low temperatures, warm rolled M-50 reaches a given hardness sooner, or at lower austenitizing temperature, than does the as-received material.

Hardness differences, or their absence, may be explained by considering the behavior of the soluble  $M_{23}C_6$  and  $M_6C$  carbides in M-50. The solvus temperatures of these carbides are 993C and 1088C [Ref. 19]. The higher temperature solvus divides the austenitizing temperature range examined into two distinct areas. In the first, 900-1088C, the  $M_{23}C_6$  or  $M_6C$  carbides are not completely dissolved in the austenite, and hardness differences are evident in Figure 9. Heating to temperatures above 1088C, into the second area, yields

TABLE III

## Hardness Test Results for Two Minute Austenitizing Time

<u>Austenitizing Temperature</u>		<u>Starting Condition*</u>	<u>Hardness (Rockwell C)</u>
<u>Nominal (C)</u>	<u>Measured (C)</u>		
900	891	A W	48 56
950	940	A W	54 60
1000	988	A W	60 63
1020	1020	A W	64 66
1050	1050	A W	65 65
1050	1043	A W	65 65
1100	1100	A W	65 64
1120	1115	A W	65 65
1150	1153	A W	63 63

\*A = As-received, W = Warm Rolled

TABLE IV

## Hardness Test Results for 1020C Austenitizing Temperature

<u>Austenitizing Time (Minutes)</u>	<u>Starting Condition*</u>	<u>Hardness (Rockwell C)</u>
0.2	A	52
	W	59
0.5	A	58
	W	63
1.0	A	61
	W	65
2.0	A	64
	W	66
5.0	A	65
	W	66
10.0	A	64
	W	65
20.00	A	64
	W	65

\*A = As-received, W = Warm Rolled

TABLE V

Hardness Test Results for 1120C Austenitizing Temperature

<u>Austenitizing Time (Minutes)</u>	<u>Starting Condition*</u>	<u>Hardness (Rockwell C)</u>
0.2	A	62
	W	66
0.5	A	65
	W	65
1.0	A	65
	W	65
2.0	A	65
	W	65
5.0	A	65
	W	65
10.0	A	64
	W	64
20.0	A	63
	W	64

\*A = As-received, W = Warm Rolled

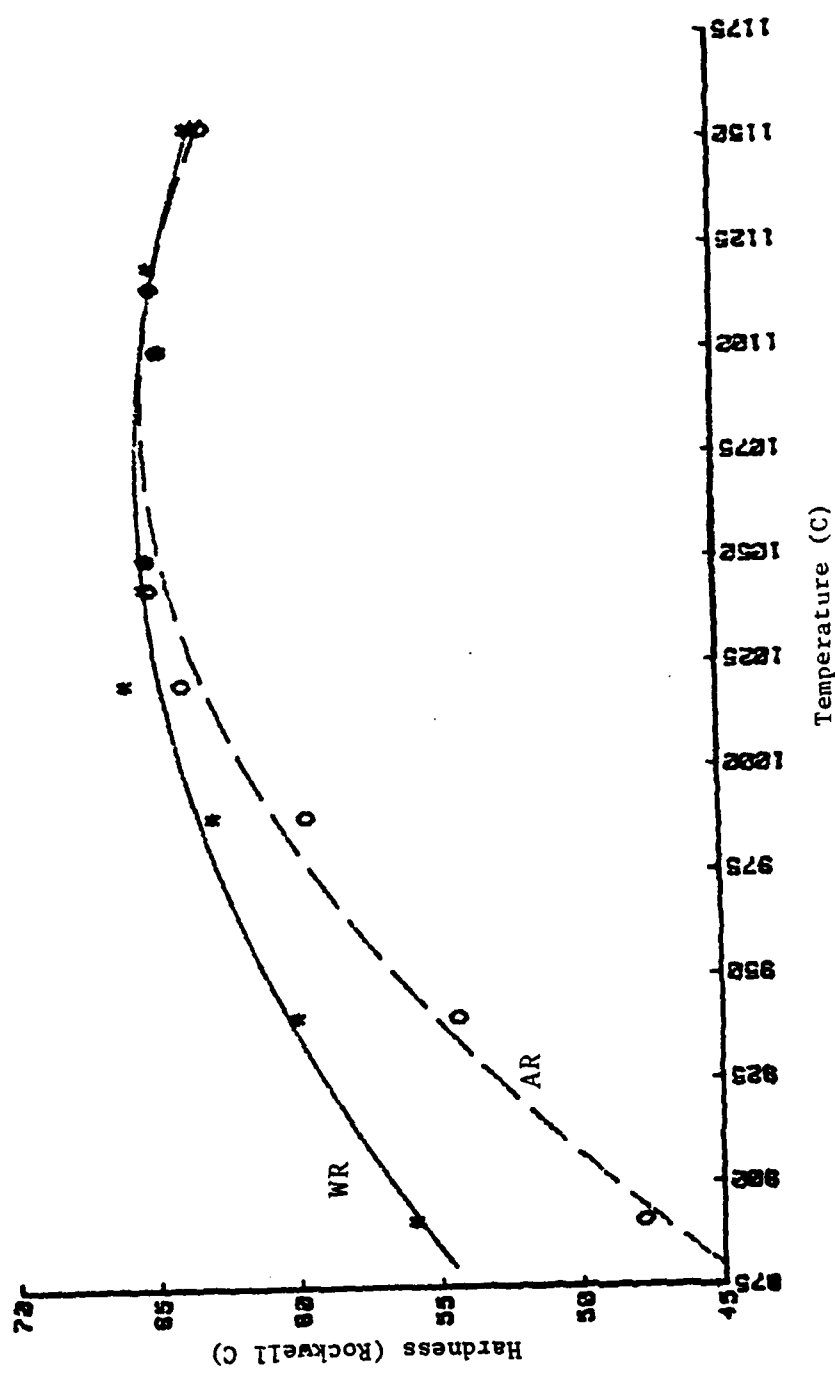


Figure 9. Hardness of Warm Rolled and As-received M-50 at Austenitizing Time Two Minutes, Varying Austenitizing Temperature.

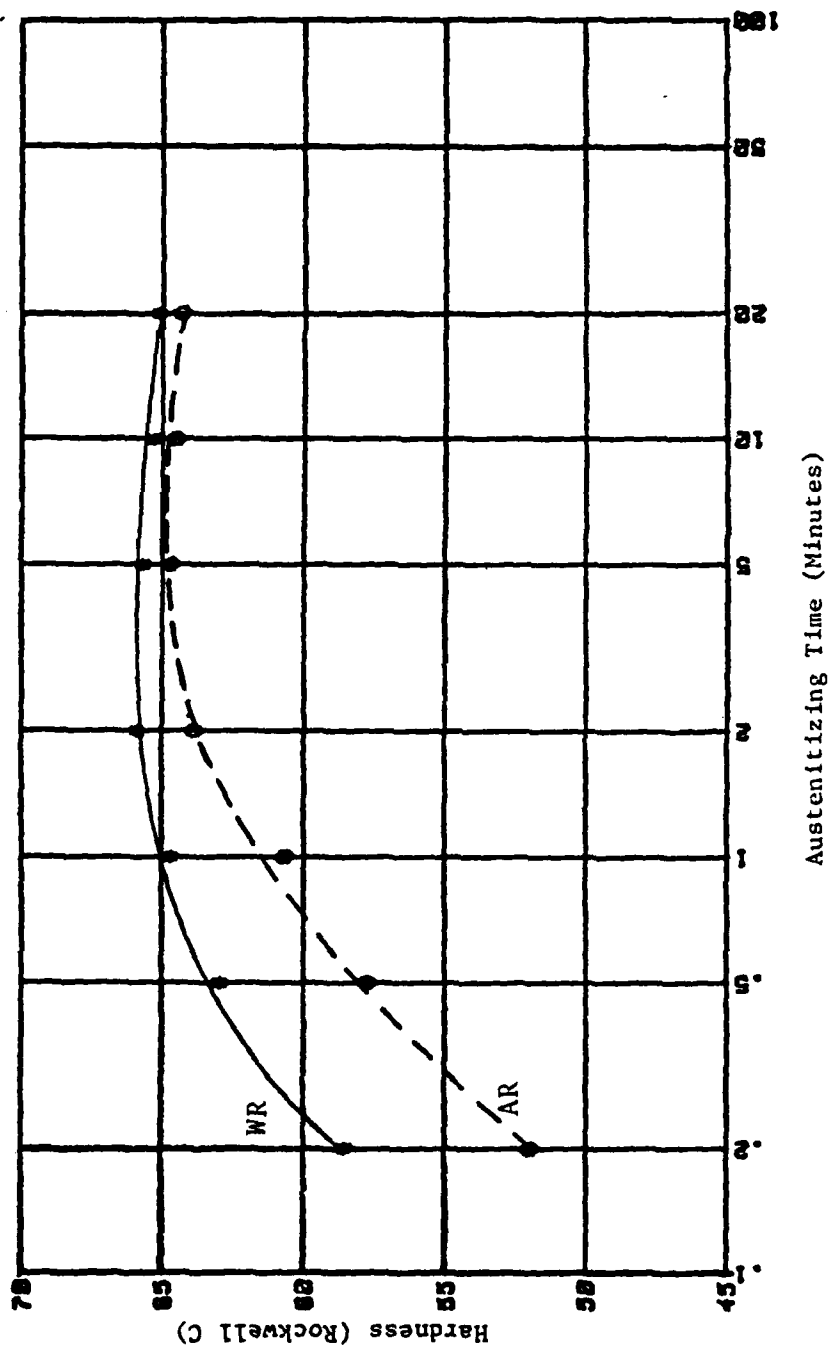


Figure 10. Hardness of Warm Rolled and As-received M-50 at Austenitizing Temperature 1020C, Varying Austenitizing Time.

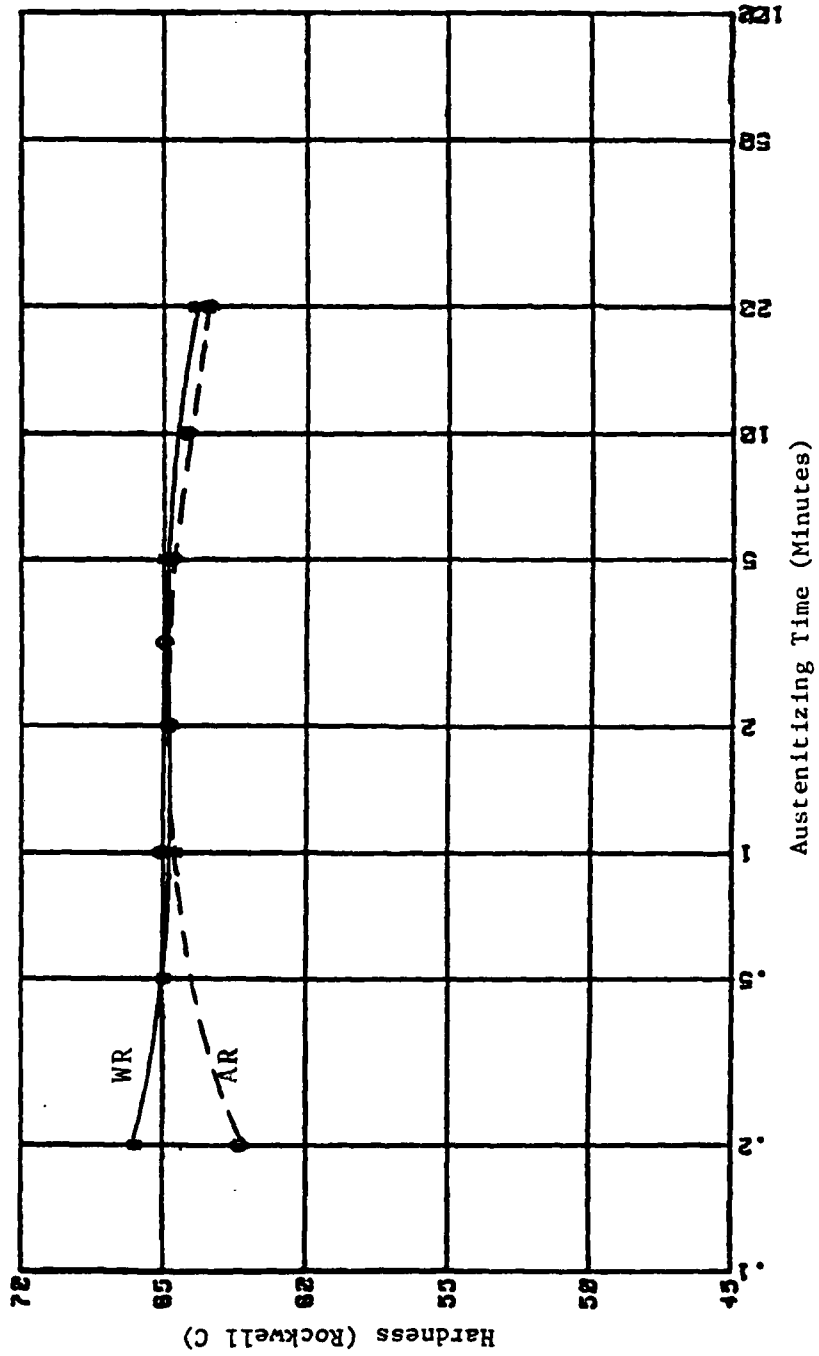


Figure 11. Hardness of Warm Rolled and As-received M-50 at Austenitizing Temperature 1120C, Varying Austenitizing Time.

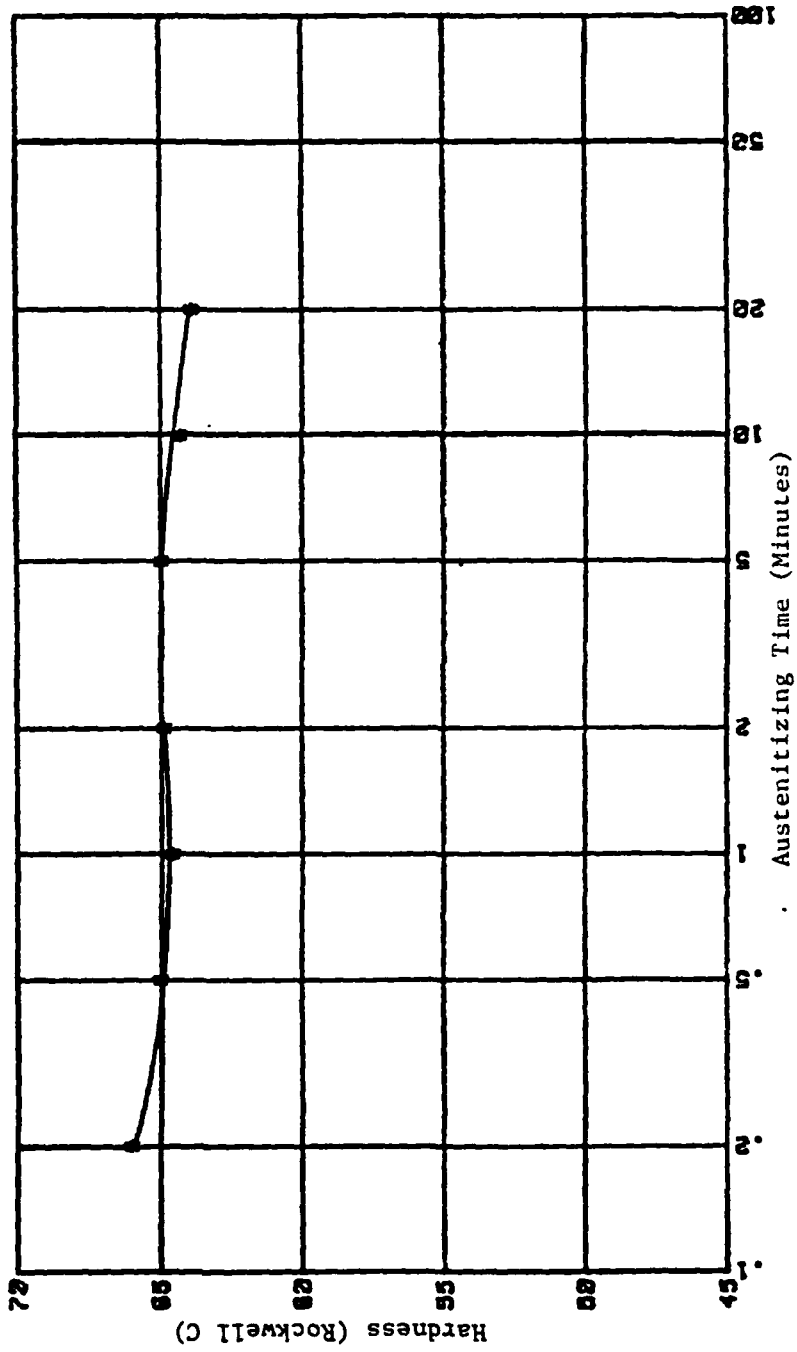


Figure 12. Hardness of Warm Rolled M-50 at Austenitizing Temperature 1120C, Varying Austenitizing Time.

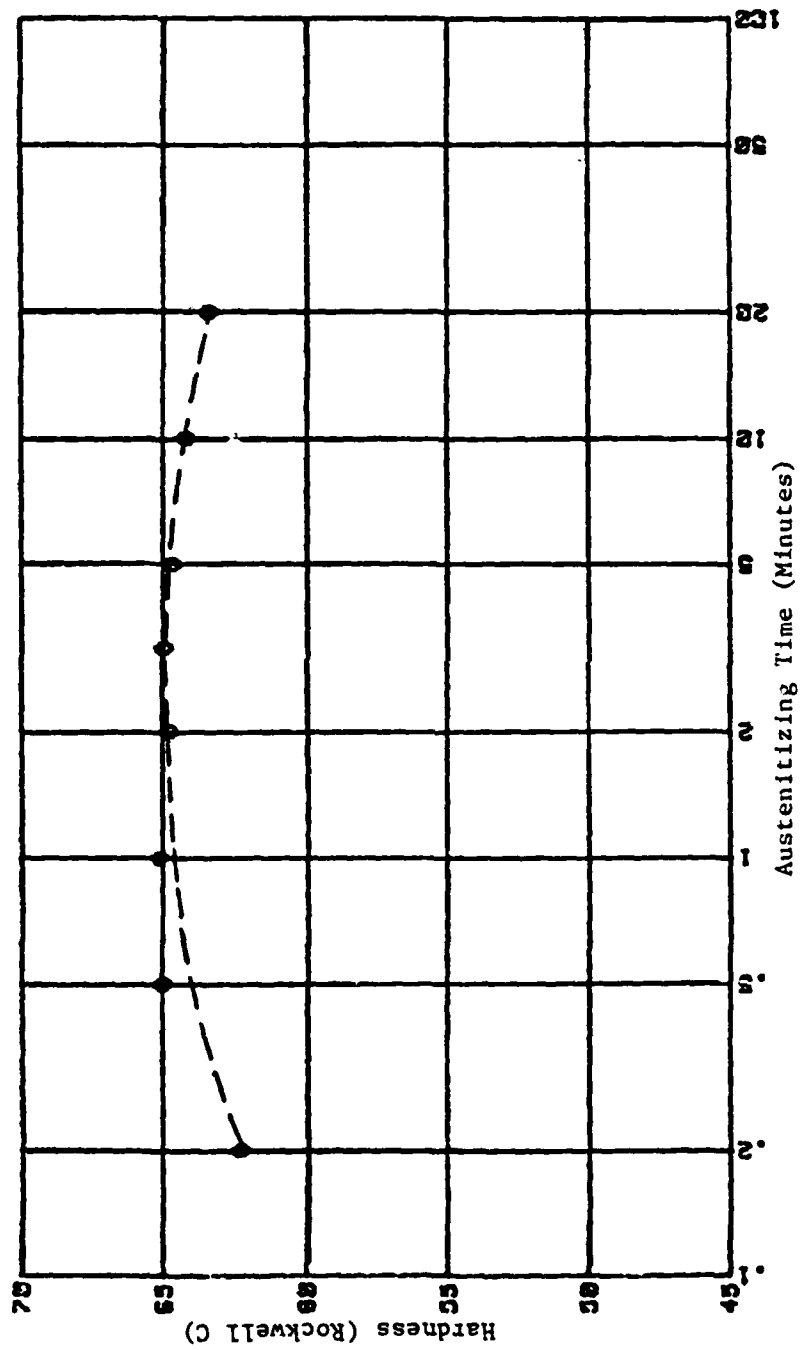


Figure 13. Hardness of As-received M-50 at Austenitizing Temperature 1120C, Varying Austenitizing Time.

an austenite in which only the insoluble carbides  $M_2C$  and  $MC$ , remain. It is in this area that the hardness curves for both the standard and warm rolled M-50 coincide (Figure 9, right side).

Below the  $M_6C$  solvus, higher hardness is attributed to a higher concentration of carbon in the matrix for warm rolled than for as-received M-50. The fine  $M_2C$  and  $MC$  carbides that precipitated during warm rolling have a smaller size and mean interparticle spacing than do the fewer, relatively large temper carbides in the as-received steel. Thus the characteristic diffusion distance is shorter after warm rolling, and the solute concentration gradients are steeper. These factors point to a greater driving force for diffusion, (based on concentration gradient), and a shorter relaxation time (proportional to the square of the diffusion distance), and therefore warm rolled M-50 will have more carbon in the austenite at any time than will its as-received counterpart. More carbon results in higher hardness.

When austenitizing for two minutes, warm rolled steel maintains its significant hardness advantage only to about 1050C. At higher temperatures, the diffusion coefficient,  $D$ , is large ( $D=D_0 \exp(-Q/RT)$ ), and diffusion of carbon and substitutional chromium and molybdenum is very rapid. The convergence at high austenitizing temperature of the warm rolled and as-received hardness versus temperature curves

may be understood if it is assumed that solutioning of soluble carbides is so fast at these temperatures that essentially all of them have been completely dissolved after two minutes in both the coarser as-received steel, and the finer, warm rolled material. The result would be the same carbon content in each, giving similar hardness, although the finer structure is retained in warm rolled M-50.

The plot of hardness versus austenitizing time for austenitizing at 1020C corroborates these conclusions. For short times, the warm rolled steel is harder than the as-received M-50, again suggesting faster solutioning of the finer carbides. An alternative hypothesis is that the reaction may be interface controlled, so that warm rolled M-50's greater carbide surface area per unit volume may explain its more rapid dissolution. Given long austenitizing times, however, when nearly all of the soluble carbides have been dissolved, the two curves are very close.

The shape of the hardness versus austenitizing time plot for warm rolled M-50 is typical for steel. The curve is generally understood to show increasing hardness with time as carbon begins to dissolve in the matrix. The peak occurs as the softening effect of retained austenite (the dominant effect for long austenitizing times) just balances the hardening effect of carbon in the matrix (dominant at short times). A surprising result, however, is that peak hardnesses in Figure 10 are attained for both starting conditions

after virtually the same austenitizing time. If carbides dissolve faster in warm rolled M-50, then the hardness peak would be expected to fall at shorter austenitizing time than that required for the as-received steel to reach its peak. The discrepancy may arise from the relative importance, at this austenitizing temperature, of the various factors which influence hardness. One possible explanation is that at 1020C microstructural refinement makes a more significant contribution to hardness than does the carbon in solution. Before a firm conclusion is possible, the amount of carbon in solid solution after different austenitizing times should be determined using X-ray techniques developed at NPS by McNelley and Garg [Ref. 21]. In addition, information concerning grain size effects is necessary, and should be obtained by analysis of transmission electron microscopy results.

For austenitizing temperatures above the  $M_6C$  solvus, hardness results resemble the right hand side of Figure 10, the series of austenitizing trials at 1020C. Once all the soluble carbides have gone into solution, matrix carbon concentrations are equal. With one possible exception, no significant difference in hardness is found between warm rolled and as-received M-50 in this temperature range. In the series of constant time austenitizing trials, the two hardness curves coincide, with both curves falling off slightly.

The drop in hardness is likely a consequence of grain growth and increased retained austenite.

The exception to the close correspondence of the hardness data for the two starting conditions occurs in the series conducted at 1120C, for the 12 second austenitizing time. Even when both the error in the austenitizing time ( $\pm 1$  second) and in hardness ( $\pm 0.5$  HRC) are taken into account, a difference of more than 2 HRC remains. (Figure 11) Again, the refinement of the warm rolled steel suggests that the difference in hardness is due to accelerated dissolution of the soluble carbides. Dissolution in warm rolled steel is so fast that solutioning is complete, even at short times, and the hardness curve is virtually constant with time (Figure 12). In contrast, the hardness curve for material heat treated from the as-received condition at short times (Figure 13), suggests that the soluble carbides in as-received material are still dissolving at 12 seconds, giving increasing matrix carbon content with time and therefore increasing hardness.

#### B. MICROSTRUCTURAL RESULTS

Optical microscopy results support those of the hardness tests in that the difference between warm rolled and as-received M-50 is most pronounced after austenitizing at lower temperatures or for shorter times. Except after very long time at high austenitizing temperature, the finer microstructure of the warm rolled steel persists after heat treatment.

Figures 14, 15, and 16 illustrate the effect of varying austenitizing temperature for a heating time of two minutes. The contrast in scale of microstructures is most striking in Figure 14. These steels were austenitized at 900C (A and B) and 1000C (C and D), below the  $M_{23}C_6$  solidus, and hence four of M-50's distinct carbides are present (the fifth, metastable  $M_2C$ , is dissolved during pre-heating). The light etching network surrounding darker areas in micrograph C of this figure is a ghost pattern that is frequently evident in the as-received M-50 and occasionally observed in warm rolled material. The pattern is an etching artifact associated with the inhomogeneous distribution of chromium near prior austenite grain boundaries. This disparity in etching response is useful in observing the warm rolled material's retention of refinement.

Micrographs A and B of Figure 14 were prepared from steel austenitized above the  $M_{23}C_6$  solvus;  $M_{23}C_6$  has dissolved into the matrix, leaving  $M_6C$ ,  $M_2C$ , and MC as distinct species. Both of these microstructures are more uniformly gray than the corresponding member of the pairs in Figure 14, suggesting that the dark patches, probably clusters of fine carbides as in Figure 3C, are more sparsely populated by those fine particles. This continues to be observed in micrographs C and D, steels austenitized above the  $M_6C$  solidus at 1100C. The two structures have etched to an even more uniform gray tone, again suggesting fewer second phase particles in the matrix.

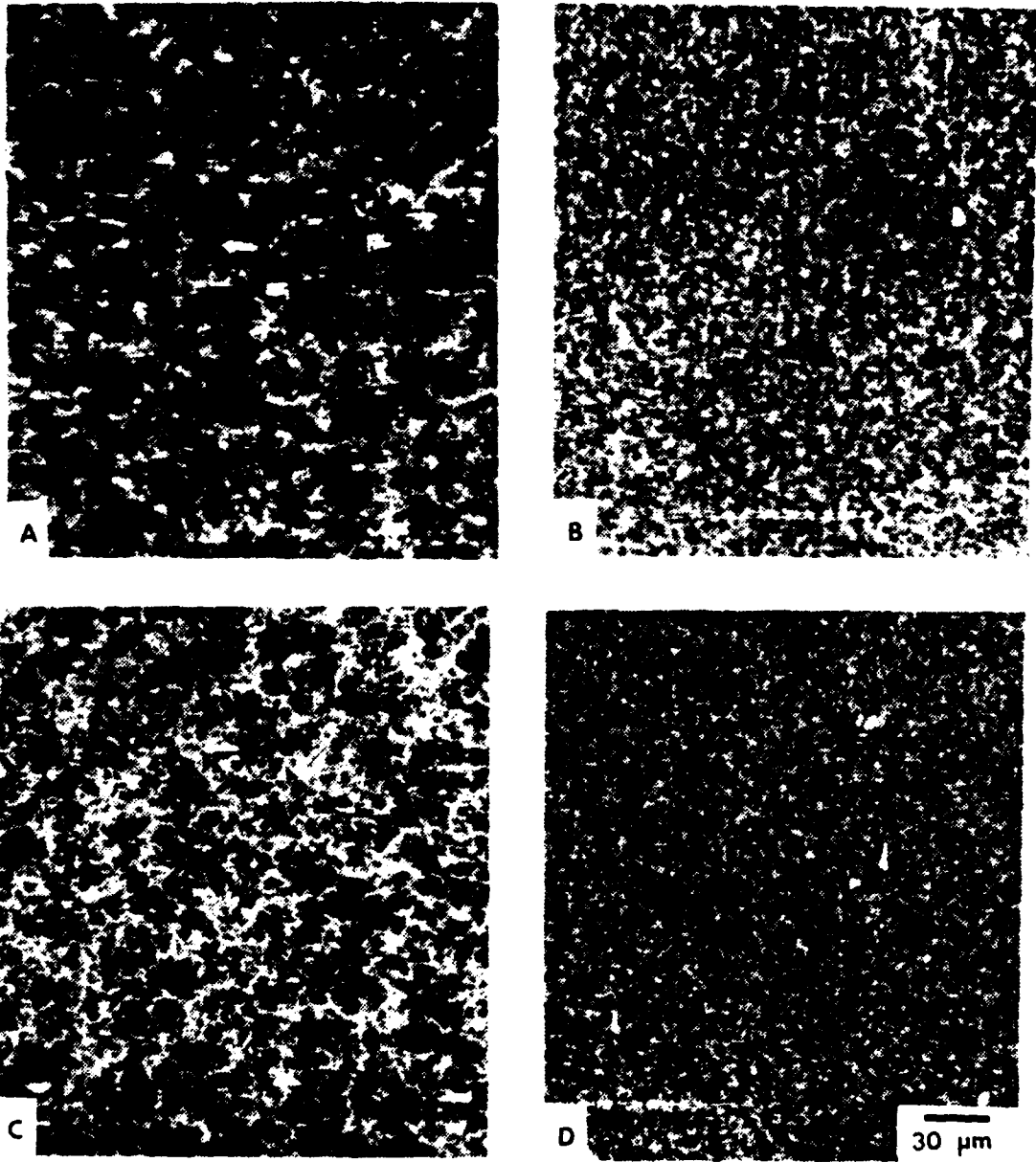


Figure 14. Comparison of Microstructures Resulting After Heat Treatment of As-received and Warm Rolled M-50 at Austenitizing Temperatures of 900C and 1000C (Optical Microscopy, 320x). A) As-received, austenitized at 900C. B) Warm rolled, austenitized at 900C. C) As-received, austenitized at 1000C. D) Warm rolled, austenitized at 1000C. Austenitizing time: 2 minutes. Carbides present:  $M_{23}C_6$ ,  $M_6C$ ,  $M_2C$ , and  $MC$ .

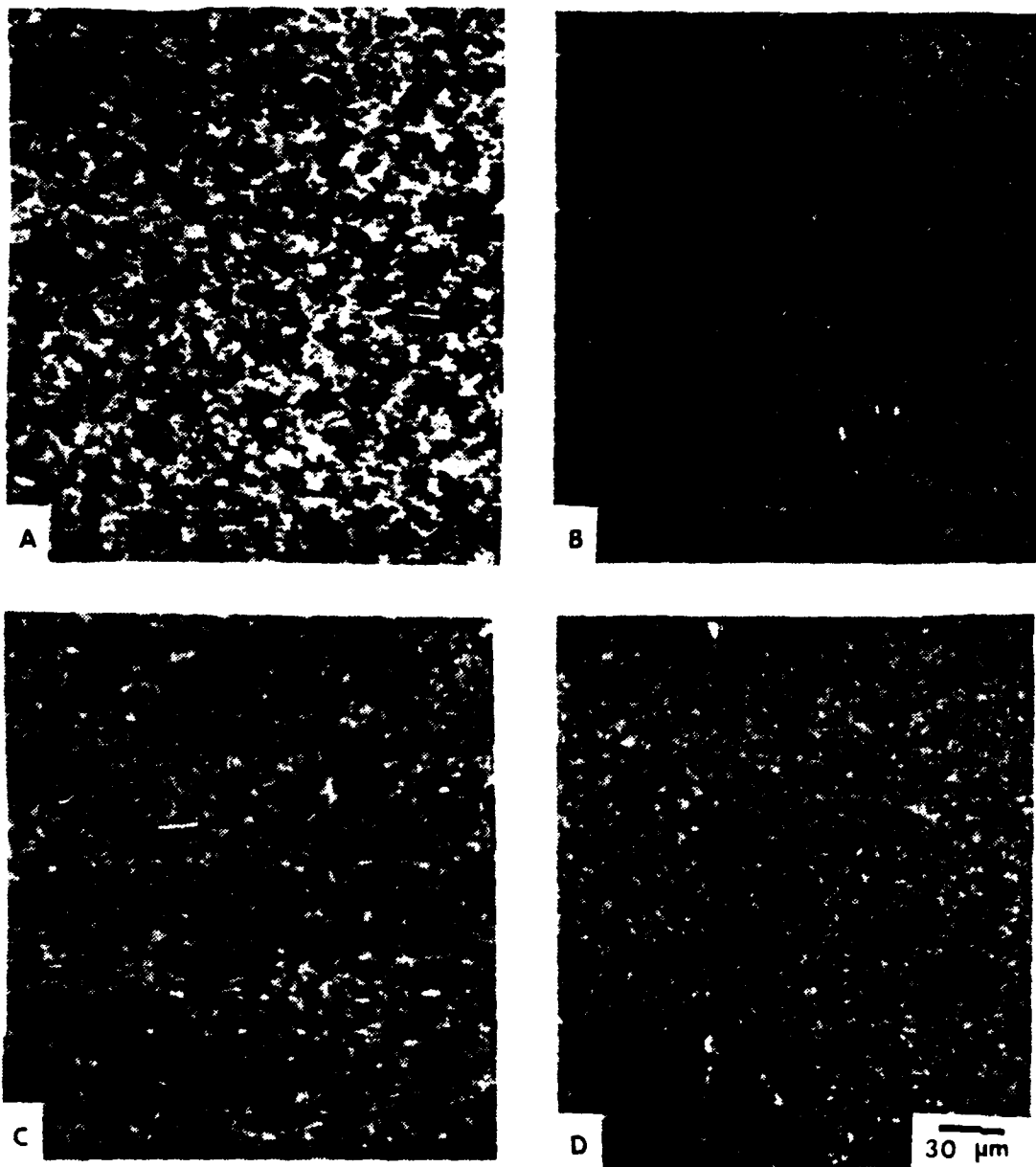


Figure 15. Comparison of Microstructures Resulting After Heat Treatment of As-received and Warm Rolled M-50 at Austenitizing Temperatures of 1050C and 1100C (Optical Microscopy, 320x). A) As-received, austenitizing at 1050C. B) Warm rolled, austenitized at 1050C. C) As-received, austenitized at 1100C. D) Warm rolled, austenitized at 1100C. Steel austenitized at 1050C contains  $M_6C$ ,  $M_2C$ , and MC (A&B); austenitizing above the  $M_6C$  solidus (1088C) only  $M_2C$  and MC remain (C&D).

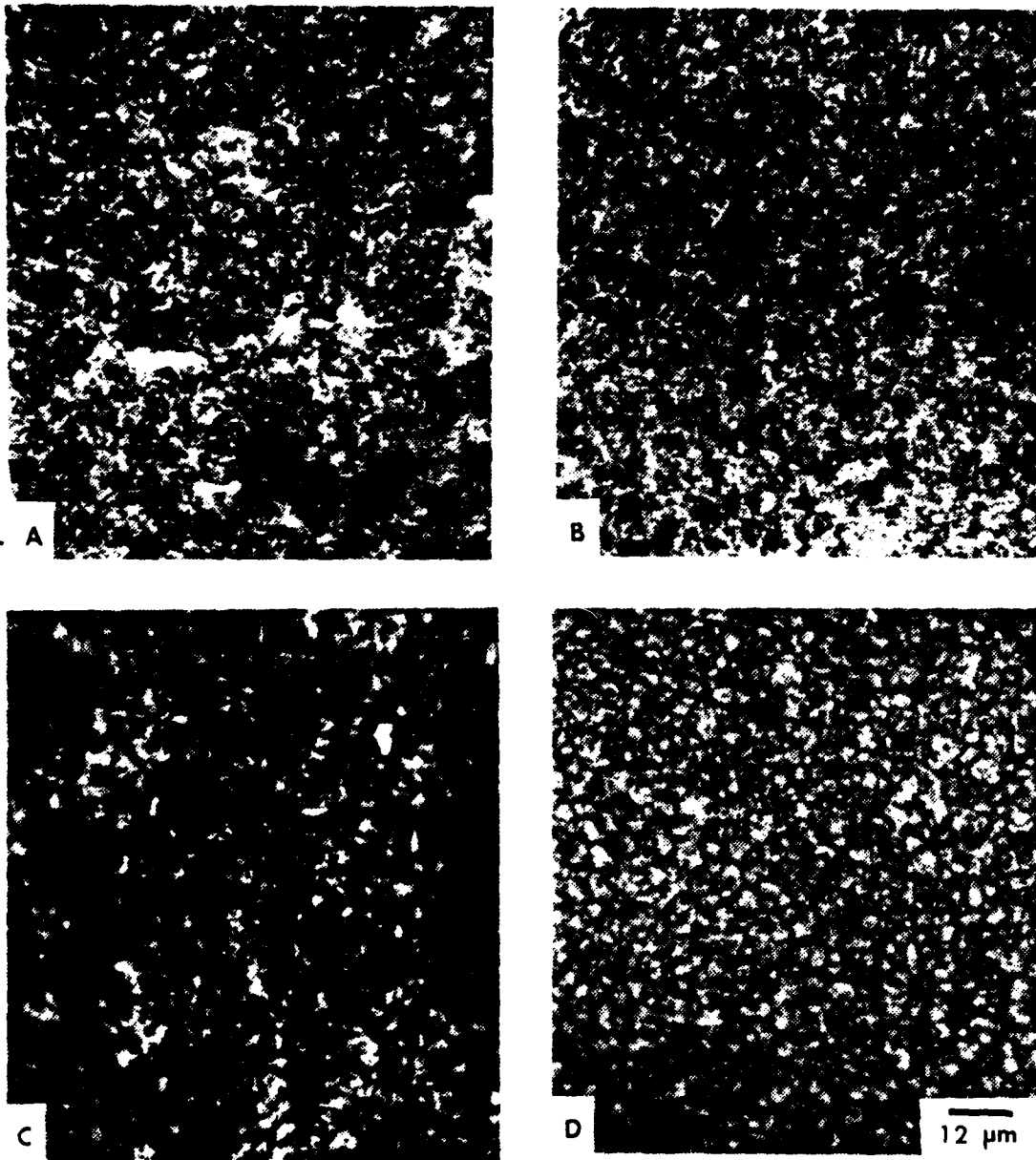


Figure 16. Comparison of Microstructures resulting After Heat Treatment of As-received and Warm Rolled M-50 at Different Austenitizing Temperatures (Optical Microscopy, 800x). A) As-received, austenitized at 900C. B) Warm rolled, austenitized at 900C. C) As-received, austenitized at 1100C. D) Warm rolled, austenitized at 1100C. Austenitizing time: 2 minutes. The finer, more homogeneous microstructure of the warm rolled starting condition persists after heat treatment.

At 1100C, the vivid difference in scale between the warm rolled and the as-received M-50 of Figure 14 is no longer apparent at this magnification. Figure 16 shows the microstructural results after austenitizing at both ends of the heat treatment range, 900C and 1100C, but this time at a magnification of 800x. After austenitizing at 900C for two minutes, Figures 16A and 16B, the dark patches seen in Figures 14A and 14B are here resolved into clusters of fine carbides similar to those observed in Figure 3, A and B. Close inspection of Figure 16C, as-received steel quenched from a two minute austenitizing treatment in 1100C, discloses the black etching network of the prior austenite grain boundaries. Although the boundaries are not clear enough to precisely determine grain size, the grains can be measured from the micrograph and converted to give a rough estimate of 15 microns. In Figure 16D, grain size can be obtained with somewhat more precision, because of its better definition of the grain boundaries. The size in this case is approximately 3.5 microns. This difference in grain size of a factor of slightly more than four is less than that in the warm-rolled condition but still notable given the high austenitizing temperature and prolonged heating time at this temperature.

The second heat treatment variable considered here was austenitizing time. Microstructures resulting from austenitizing at 1020C are seen in Figures 17, 18, and 19.

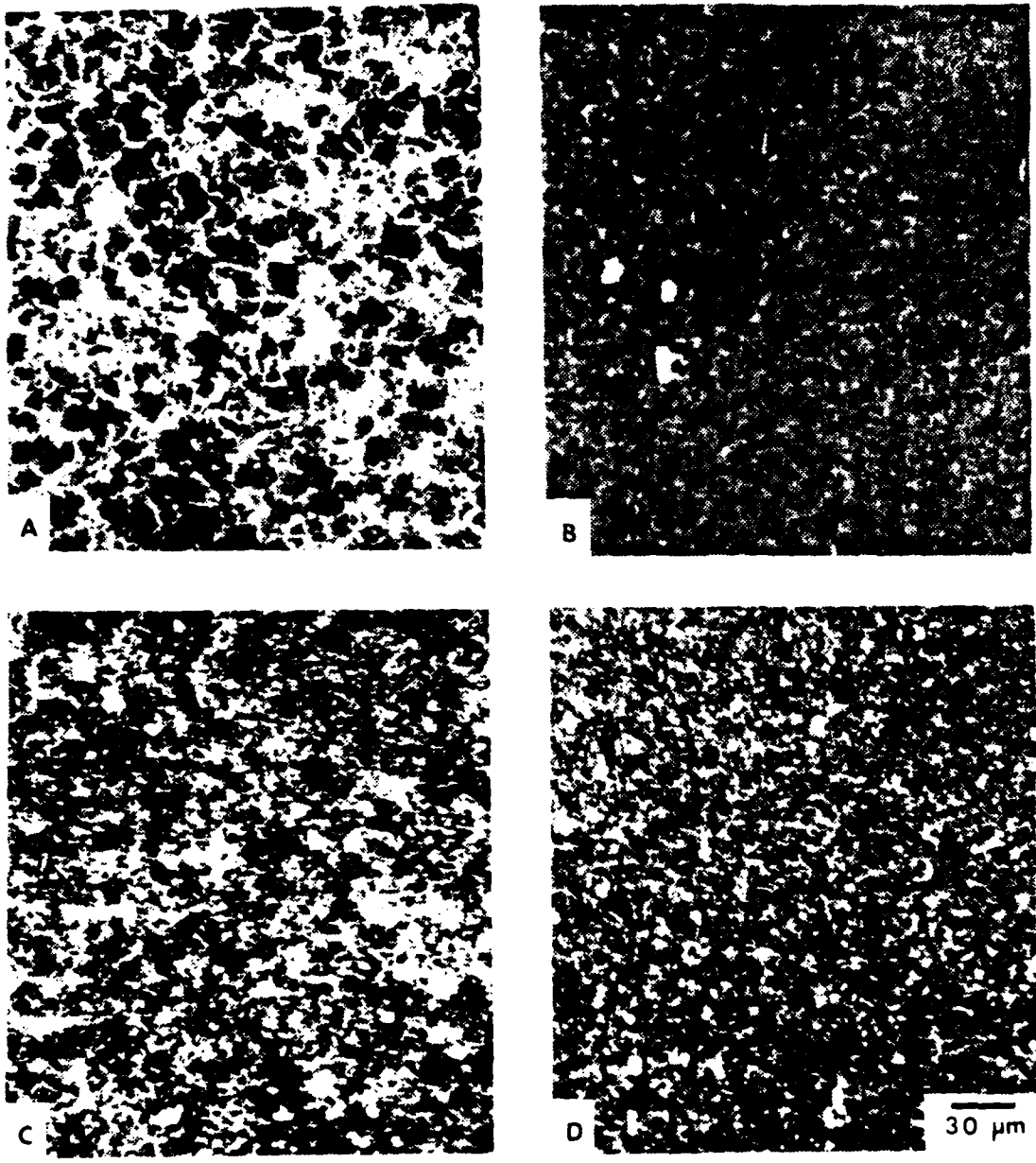


Figure 17. Comparison of Microstructures Resulting After Heat Treatment of As-received and Warm Rolled M-50 for Short Austenitizing Times at 1020C (Optical Microscopy, 320x). A) As-received, austenitized for 1/2 minute. B) Warm rolled, austenitized for 1/2 minute. C) As-received, austenitized for 2 minutes. D) Warm rolled, austenitized for 2 minutes. Carbides present:  $M_6C$ ,  $M_2C$ , and  $MC$ . Micrographs for the 2 minute austenitizing time may be compared with Figure 14.

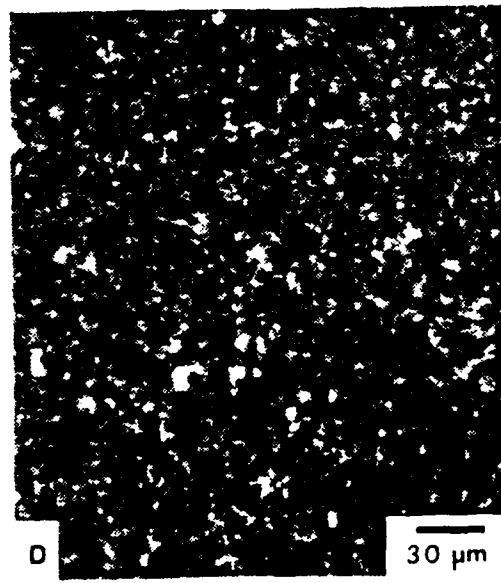
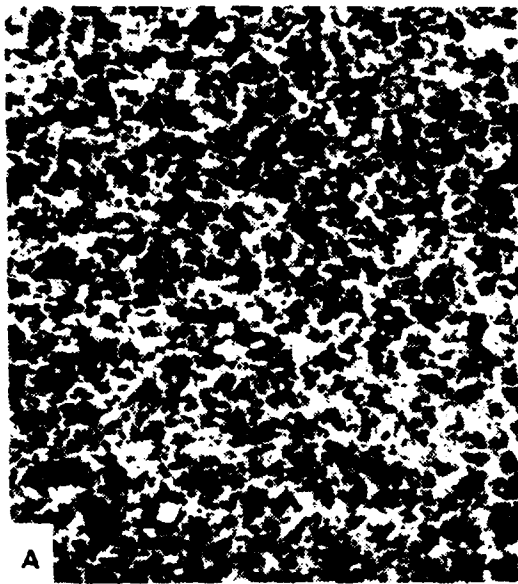


Figure 18. Comparison of Microstructures Resulting After Heat Treatment of As-received and Warm Rolled M-50 for Long Austenitizing Times at 1020C (Optical Microscopy, 320x). A) As-received, austenitized for 5 minutes. B) Warm rolled, austenitized for 5 minutes. C) As-received, austenitized for 10 minutes. D) Warm rolled, austenitized for 10 minutes. Carbides present:  $M_6C$ ,  $M_2C$ , and  $MC$ .

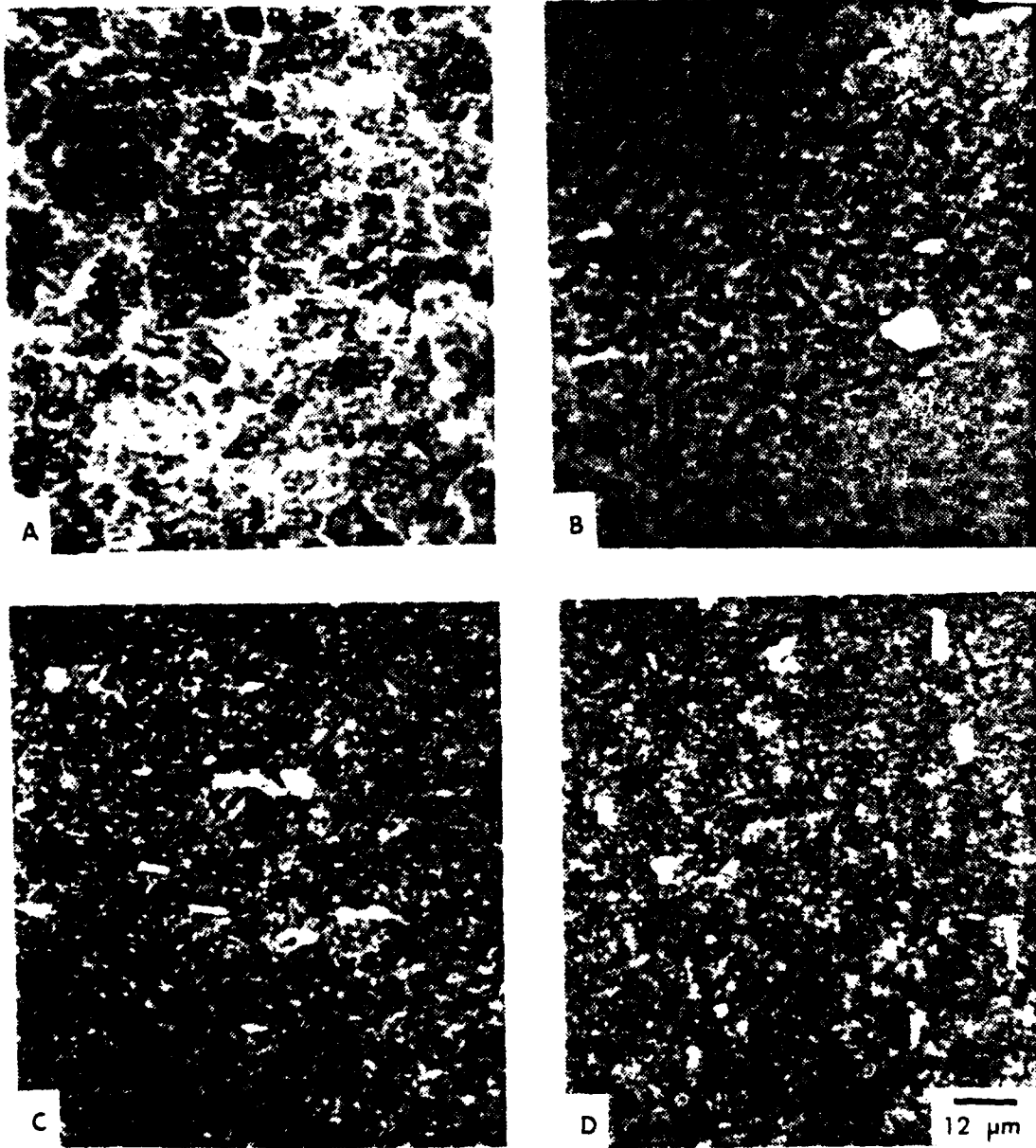


Figure 19. Comparison of Microstructures Resulting After Heat Treatment of As-received and Warm Rolled M-50 for Different Austenitizing Times at 1020C (Optical Microscopy, 800x). A) As-received, austenitized  $\frac{1}{2}$  minute. B) Warm rolled, austenitized  $\frac{1}{2}$  minute. C) As-received, austenitized 10 minutes. D) Warm rolled, austenitized 10 minutes. For each austenitizing time, the microstructures are very similar, and that resulting from the warm rolled steel is finer in scale.

All twelve micrographs in these three figures depict microstructures containing  $M_6C$ ,  $M_2C$ , and  $MC$  carbides.

For a short austenitizing time of 30 seconds at 1020C (Figure 17, A and B), pronounced refinement is again evident (compare Figure 14, A and B). The ghost pattern described in connection with Figure 14 is clear in the as-received steel of micrograph A, and is also discernible in the warm rolled material, micrograph B.

A gap in the series of two minute heat treatments is filled by comparing results depicted in Figures 18C and 18D, microstructures resulting after heat treatment for two minutes at 1020C, with results shown in Figure 14, for austenitizing at 900 and 1000C. These two micrographs for 1020C show less difference in scale than was seen in either of the sets of Figure 14, and yet the structures are also less alike than the pairs shown in Figure 15, which were austenitized at still higher temperatures.

The trend demonstrated by varying austenitizing temperature is convergence of microstructures as austenitizing temperature increases. The same trend can be found on examination of the effect of varying time at 1020C austenitizing temperature. Looking at either the set of as-received microstructures or those produced from a warm rolled starting condition, the steels increase in both microstructural homogeneity and hardness with increasing austenitizing time. In fact, the microstructures of Figure 18B and 18D, warm rolled

M-50 austenitized at 1020C for 5 and 10 minutes, are virtually indistinguishable. Matching hardnesses are also noted, within the limits of measurement error: the 5 minute sample is 66 HRC, and austenitizing for 10 minutes gives 65 HRC. Warm rolled steel may thus be considered more "tolerant" of variations in processing. In other words, the heat treatment of warm rolled M-50 need not be so closely controlled to produce a given result as must processing from the as-received condition, since doubling the austenitizing time here, at a temperature known only to  $\pm 7.7C$  [Ref. 22], yields the same product.

Convergence of the microstructures after long austenitizing times is illustrated by Figure 19, which repeats the pattern of readily apparent difference in scale at short austenitizing times (30 seconds, 1020C, micrographs A and B), and only a very slight difference, if any, for long austenitizing times (10 minutes, 1020C, micrographs C and D). Magnification here is 800x.

Hardness results for the series of varying time austenitizing trials at 1120C predict that differences in microstructures would be found only at short austenitizing times, and that any difference found would be slight. Figures 20, 21, and 22 show the microstructures of both starting conditions after quenching. Only the insoluble carbides,  $M_2C$  and MC, are present.

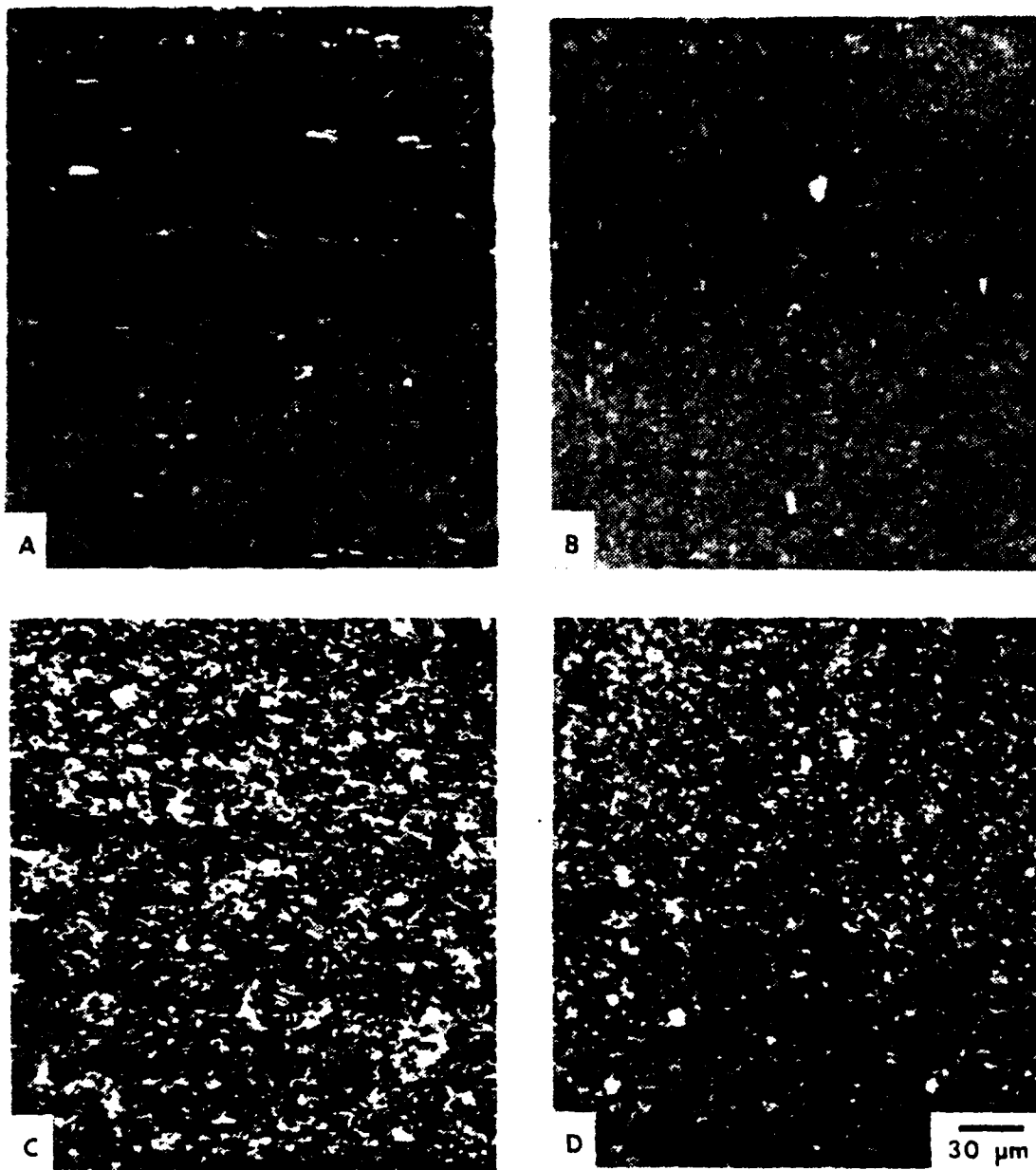


Figure 20. Comparison of Microstructures Resulting After Heat Treatment of As-received and Warm Rolled M-50 for Short Austenitizing Times at 1120C (Optical Microscopy, 320x). A) As-received, austenitized for  $\frac{1}{2}$  minute. B) Warm rolled, austenitized for  $\frac{1}{2}$  minute. C) As-received, austenitized for 2 minutes. D) Warm rolled, austenitized for 2 minutes. Carbides present:  $M_7C_3$  and MC. Micrographs for the 2 minute austenitizing time may be compared with Figure 15.

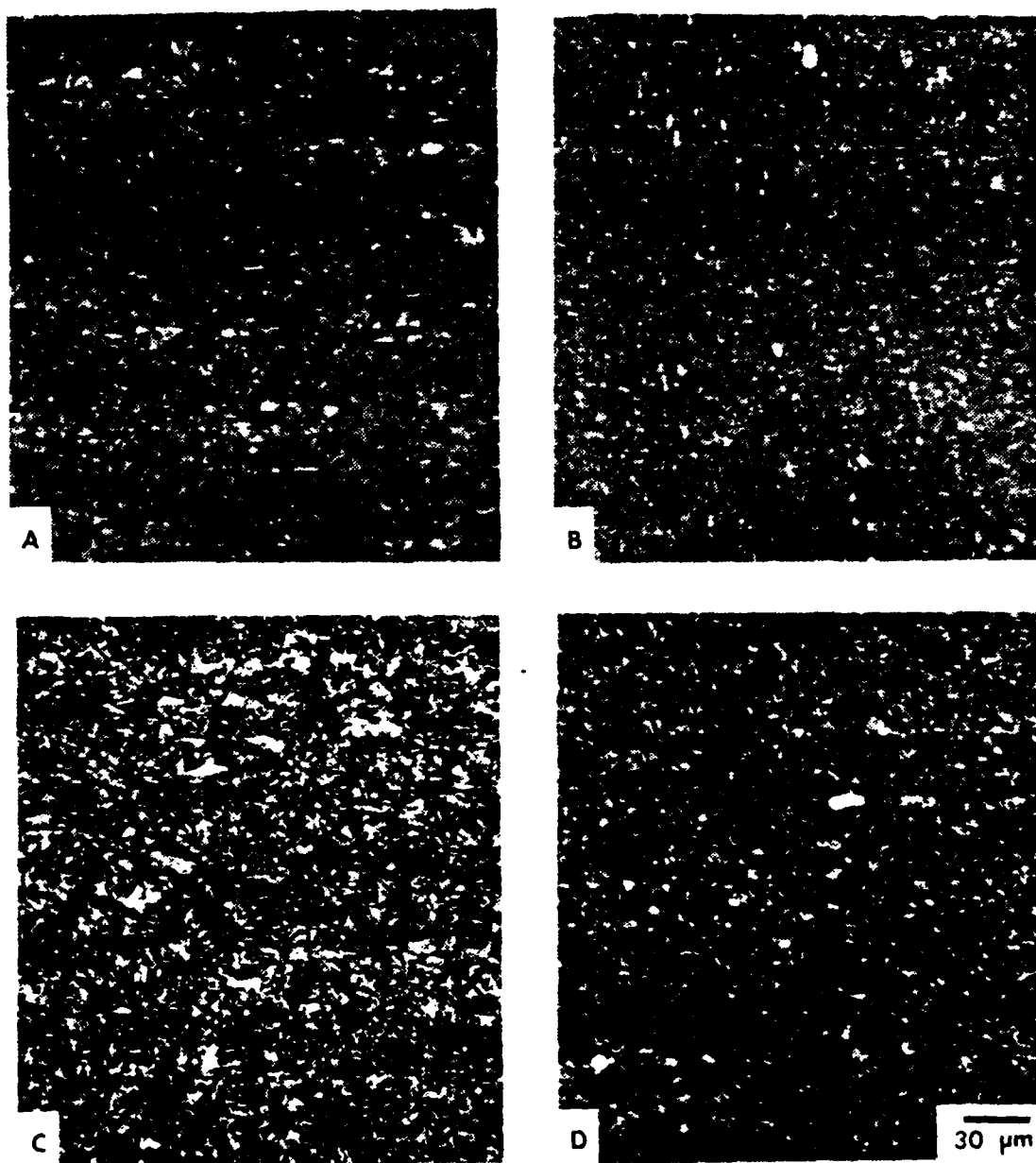


Figure 21. Comparison of Microstructures Resulting After Heat Treatment of As-received and Warm Rolled M-50 for Long Austenitizing Times at 1120C (Optical Microscopy, 320x). A) As-received, austenitized for 5 minutes. B) Warm rolled, austenitized for 5 minutes. C) As-received, austenitized for 10 minutes. D) Warm rolled, austenitized for 10 minutes. Carbides present: MC and M<sub>2</sub>C.

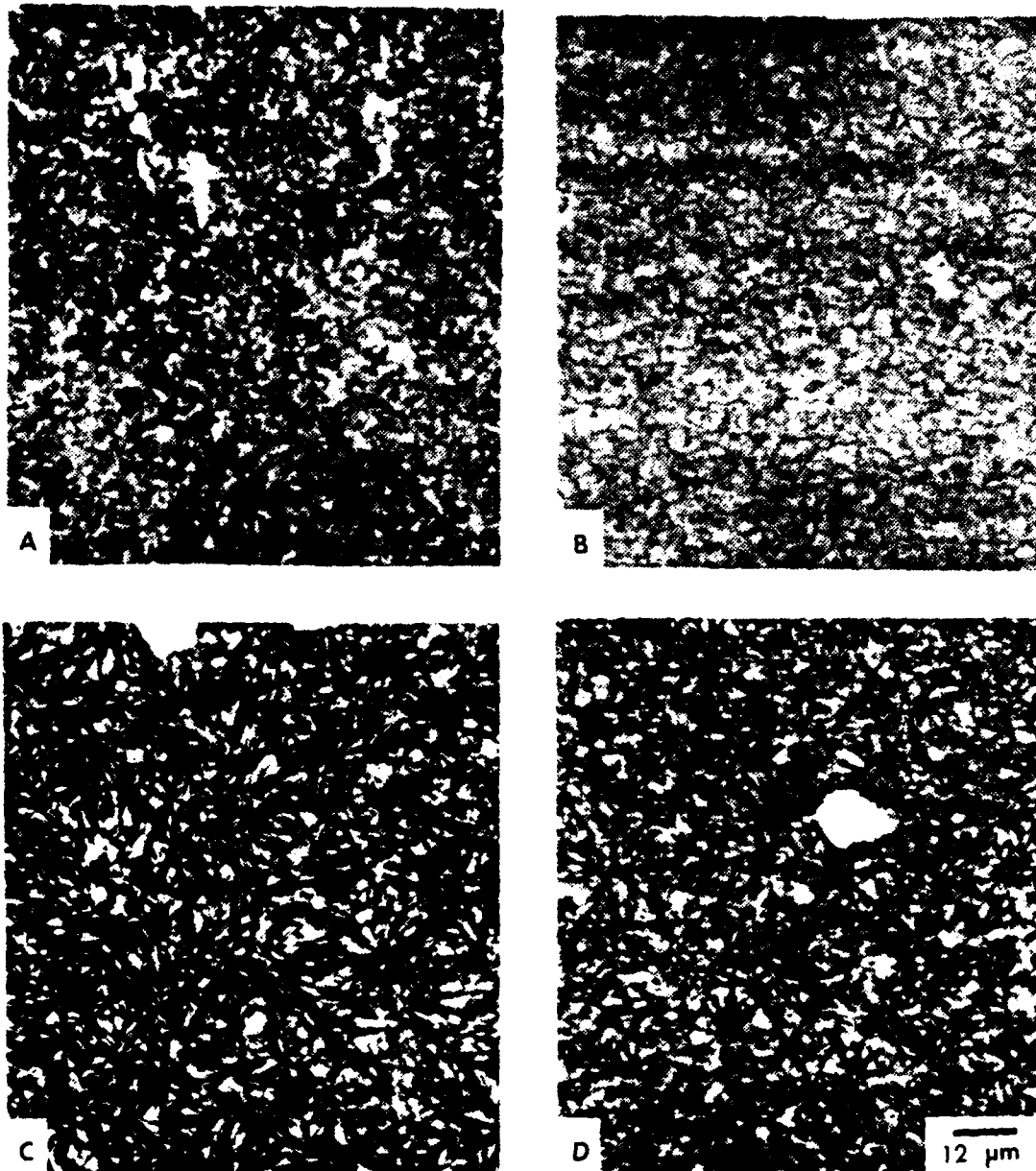


Figure 22. Comparison of Microstructures Resulting After Heat Treatment of As-received and Warm Rolled M-50 for Different Austenitizing Times at 1120C (Optical Microscopy, 800x). A) As-received, austenitized  $\frac{1}{2}$  minute. B) Warm rolled, austenitized  $\frac{1}{2}$  minute. C) As-received, austenitized 10 minutes. D) Warm rolled, austenitized 10 minutes. Carbides present: M<sub>6</sub>C and MC. Microstructures in C and D consist of plate martensite, retained austenite, and insoluble carbides. They illustrate the convergence of the microstructures for long austenitizing times and high temperatures.

At 320x, there is no apparent difference in any of the four pairs of steels in Figures 20 and 21. The slight difference between the two steels hardened on 30 seconds at 1120C is evident only after raising the magnification to 800x, Figure 22, A and B. Even this higher magnification discloses little difference in the microstructures of the pair held at high temperature for 10 minutes.

The significance of the hardness difference at the 0.2 minute point on the curve is confirmed by the microstructures of Figure 23. Once again, at 320x, there is a striking difference between the coarse as-received steel with its distinct ghost pattern and the refined, much more uniform structure of the warm rolled M-50. At longer austenitizing times, both microstructure and hardness converge, but for this very short period at high temperature (a shorter interval than the 20-30 seconds required to get a steady temperature read-out on the digital thermometer), the finer carbides again dissolve faster and to give a higher hardness.

The microstructure of M-50 quenched from two or more minutes at 1100, and 1120 and 1150C consists of insoluble carbides, retained austenite, and plate martensite [Refs. 24, 25], for both the warm rolled and as-received starting conditions. Optical microscopy is inadequate to determine the constituents of those microstructures resulting from other austenitizing conditions. Although investigation of the microstructures was undertaken using the scanning electron

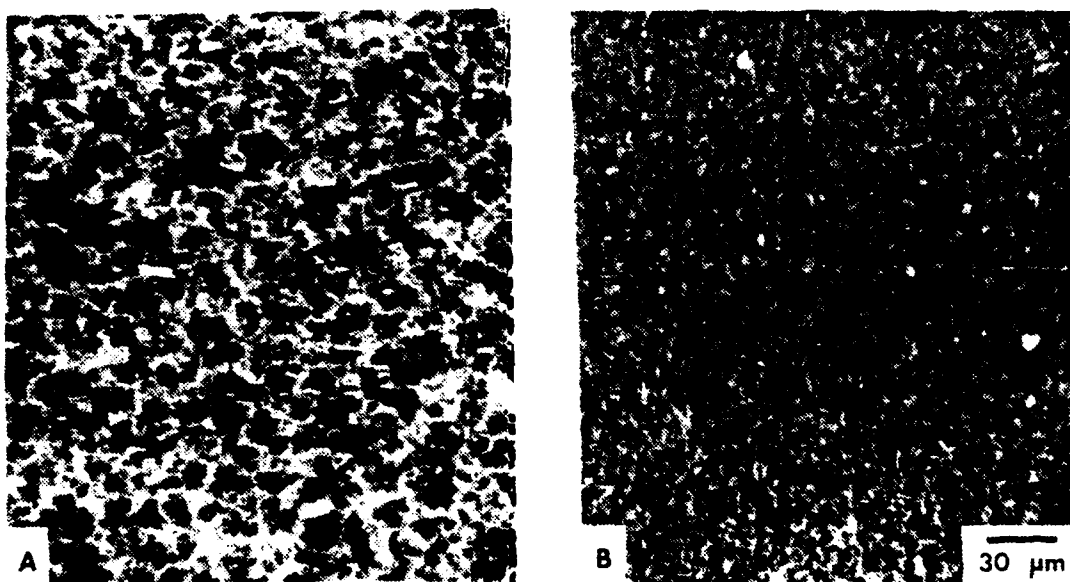


Figure 23. Comparison of Microstructures Resulting After Heat Treatment of As-received and Warm Rolled M-50 for Austenitizing Time 12 Seconds at 1120C (Optical Microscopy, 320x). A) As-received. B) Warm rolled. The degree of difference in scale between the two microstructures is similar to that of Figure 14, A and B.

microscope at 2000x, no new information resulted; transmission electron microscopy (TEM) should be used to examine microstructures from representative austenitizing conditions. Using TEM, it should be possible to investigate the hypothesis that hardened M-50 microstructures undergo a transition from lath to plate martensite with increasing austenitizing temperature similar to that reported by Nakazawa and Kraus for 52100 steel [Ref. 26].

### C. COMPARISON OF AUSFORMING AND WARM ROLLING

In 1967, Bamberger reported using thermomechanical processing to extend the rolling contact fatigue life of M-50 [Ref. 27]. He found that ausforming, a process in which the steel was deformed in the metastable austenitic region of its Time-Temperature-Transformation (TTT) curve (Figure 24), could give an improvement in rolling contact fatigue life of up to 600% for sufficiently large deformations. Ausforming is possible only for material with a TTT curve like M-50's in which the large bay signifies a region where austenite is stable for long times at intermediate temperature. Thus there is time for the steel to be deformed prior to its transformation to martensite.

Bamberger austenitized at 2150F (1176C), air quenched to 1050F (565C), then worked the M-50 to a final reduction in area of approximately 40, 70, and 80 percent. Air cooling to ambient temperature followed, with subsequent tempering for 2 hours at 600F (315C) to prevent cracking. Tempering

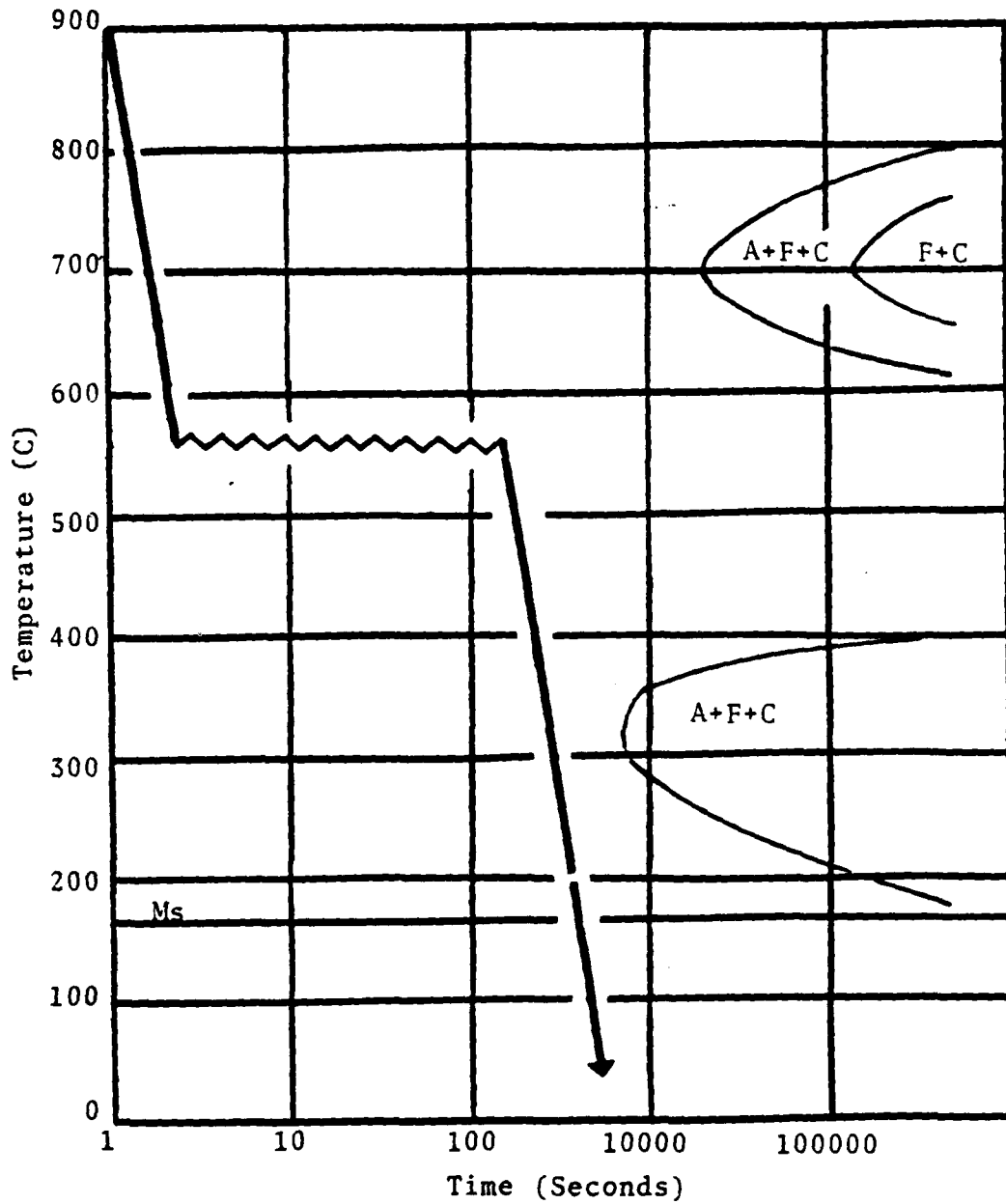


Figure 24. Time-Temperature-Transformation Diagram for M-50 Steel. The ausforming procedure carried out by Bamberger [Ref. 23] is illustrated.

studies were then conducted to determine the effect of ausforming on secondary hardening. Test specimens were then run on a General Electric Rolling Contact rig to determine rolling contact fatigue life. Results of this work showed that the improvement in rolling contact fatigue life brought about by ausforming was greater with greater deformation. The size of insoluble carbides was not reduced by ausforming, suggesting that rolling contact fatigue life is increased due to a change in the matrix, not by refinement of the  $M_2C$  and MC insoluble carbides.

Warm rolling, at first glance, appears very similar to ausforming. Sherby's process may also utilize working the steel in its metastable austenite region to a large reduction in area. As in ausforming, during warm rolling strain induced precipitation occurs during deformation which results in small, uniformly dispersed temper carbides. Both processes are applied to initially spheroidize-annealed steel, and both attempt to improve bearing reliability by improving rolling contact fatigue life.

Consideration of the details and consequences of the two procedures, however, leads to the conclusion that their differences are more significant than their resemblance. Most important is the point in the bearing manufacturing sequence at which the two processes are designed to be used. Warm rolling was interposed as an intermediate step in this work because M-50 is available from the manufacturer only as

spheroidize-annealed material and it was necessary to back it out of that condition. In industrial practice, warm rolling would take place before the steel was delivered to the bearing vendor for fabrication into the finished product. Warm rolled M-50's ferrite matrix with spheroidized carbides is soft (about 30 HRC) and superplastic, so normal manufacturing methods can easily be employed. Warm rolling's primary purpose in bearing applications is to increase fracture toughness by providing a refined microstructure onto the final, heat treated condition, though it may be also carry a bonus in rolling contact fatigue life. Ausforming, on the other hand, integrates deformation with the final hardening treatment. It requires revamped manufacturing techniques because it produces martensitic M-50 of 63-64 HRC [Ref. 28], which is not easily machined. Ausforming also differs in that its focus is extension of rolling contact fatigue life. It is not directed at improving fracture toughness, and it would not be expected to have this effect, since it affords no significant refinement in microstructure. Of these two thermomechanical processes, only warm rolling may carry benefits that permit its application to advanced gas turbine bearing operation at high DN.

#### IV. CONCLUSIONS AND RECOMMENDATIONS

Conclusions of this study of the heat treatment response of warm rolled M-50 steel in comparison to as-received steel may be summarized as follows:

1. The finer microstructure of warm rolled M-50 persists after heat treatment.

2. Differences between the two conditions are most pronounced when the austenitizing treatment is short, or occurs at low temperature. Microstructures and hardnesses resulting after long austenitizing times tend to come together, particularly if treated at high austenitizing temperature.

3. At a given austenitizing temperature below the  $M_6C$  solidus, warm rolled M-50 is harder than the as-received material (or, a given hardness may be achieved by austenitizing warm rolled M-50 at a lower temperature than that required for the as-received material). Hardness differences appear to be a consequence of warm rolled M-50's finer soluble carbides dissolving faster to give more carbon in the matrix. Austenitizing above the  $M_6C$  solidus results in little or no difference in hardness, except for very short austenitizing times.

A more complete understanding of warm rolled M-50 will be possible after additional work is completed:

1. Use transmission electron microscopy to determine microstructural constituents of M-50 austenitized below 1100C, and to provide grain size information for all austenitizing conditions.

2. Measure the percent carbon in austenite for selected austenitizing conditions using X-ray techniques.

3. Conduct rolling contact fatigue and fracture toughness testing.

## LIST OF REFERENCES

1. A. F. Wright Aeronautical Laboratories Report AFWAL-TR-83-2022, Improved Fracture Toughness Bearings, by E. N. Bamberger, B. L. Averbach and R. K. Pearson, p. 10, April 1983.
2. NASA Technical Memorandum NASA TM X-71441, Rolling Element Bearings: A Review of the State of the Art, by W. J. Anderson and E. V. Zaretsky, p. 2, October 1973.
3. Bamberger, pp. 13, 25.
4. Bamberger, pp. 18-25.
5. Rescalvo, J. A., Fracture and Fatigue Crack Growth in 52100, M-50, and 18-4-1 Bearing Steels, Ph.D. Thesis, Massachusetts Institute of Technology, Boston, 1979.
6. Hertzberg, R. W., Deformation and Fracture Mechanics of Engineering Materials, pp. 257, 356-362, John Wiley and Sons, 1976.
7. Metals Handbook, 9th ed., v. 4, p. 609, American Society for Metals, 1980.
8. Rescalvo, J. A. and Averbach, B. C., "Fracture and Fatigue in M-50 and 18-4-1 High Speed Steels," Metalurgical Transactions, v. 10A, pp. 1270-1284, September 1979.
9. Third Semi-Annual Progress Report to Advance Progress Research Agency Under Grant DAHC-15-73-G15, Superplastic-Ultra High Carbon Steels, Stanford University Press, by O. D. Sherby and others, February 1975.
10. Sherby, O. D. and others, "Development of Fine Spheroidized Structures by Warm Rolling of High Carbon Steels," Transactions of the American Society for Metals, v. 62., pp. 575-580, 1969.
11. McCauley, J. F., The Influence of Prior Warm Rolling on Fracture Toughness of Heat Treated AISI 52100 Steel, M.S. Thesis, Naval Postgraduate School, Monterey, 1980.
12. Larson, K. R., Jr., Thermomechanical Processing of M-50 Steel, M.S. Thesis, Naval Postgraduate School, Monterey, 1983.

13. Bridge, J. E., Jr., Maniar, G. N., and Philip, T. V., "Carbides in M-50 High Speed Steel," Metallurgical Transactions, v. 2, pp. 2209-2214, August 1971.
14. Metals Handbook, v. 4, pp. 561-562.
15. Latrobe Steel Company Data Sheet MV-1 VAC-ARC, Latrobe, Pennsylvania.
16. Annual Book of ASTM Standards, part 10, American Society for Testing and Materials, 1975.
17. Metals Handbook, 8th edition, v. 8, p. 64, American Society for Metals, 1964.
18. Ibid., p. 66.
19. Millsop, R., "A Survey of Austenite Grain Size Measurements," in Doane, D. V. and Kirkaldy, J. S., Hardenability Concepts with Applications to Steel, p. 316, American Institute of Mining, Metallurgical and Mechanical Engineers, 1978.
20. Annual Book of ASTM Standards, part 11, American Society for Testing and Materials, 1975.
21. McNelley, T. R. and Garg, A., Naval Postgraduate School, Monterey, private communication, 1983.
22. Omega Engineering, Incorporated, Complete Temperature Measurement Handbook, p. T-11, 1983.
23. Mukherjee, T., "Physical Metallurgy of High Speed Steels," in Materials for Metal Cutting, pp. 80-96, Institute of Iron and Steel, 1970.
24. Sunada, H., Wadsworth, J. Lin, J. and Sherby, O. D., "Mechanical Properties and Microstructures of Heat-Treated Ultra High Carbon Steels," Materials Science and Engineering, v. 39, pp. 35-40, 1979.
25. Nakazawa, K. and Krauss, G., "Microstructure and Fracture of 52100 Steel," Metallurgical Transactions, v. 9A, pp. 681-689, May 1978.
26. Bamberger, B. L., "Effect of Ausforming on the Rolling Contact Fatigue Life of a Typical Bearing Steel," Journal of Lubrication Technology, v. 1, pp. 63-75, January 1967.

INITIAL DISTRIBUTION LIST

	No. Copies
1. Defense Technical Information Center Cameron Station Alexandria, Virginia 22314	2
2. Library, Code 0142 Naval Postgraduate School Monterey, California 93943	2
3. Department Chairman, Code 69 Department of Mechanical Engineering Naval Postgraduate School Monterey, California 93943	1
4. Dr. T. R. McNelley, Code 69 Department of Mechanical Engineering Naval Postgraduate School Monterey, California 93943	5
5. LT Elizabeth V. Bres, USN 8187 Lariat Trail N.W. Bremerton, Washington 98310	2
6. Commander (Attn: Dan Poggoshev) Naval Air Propulsion Center P.O. Box 7176 Trenton, New Jersey 08628	2

— 88  
DTIC